AMERICAN SOCIETY FOR MICROBIOLOGY | Journal of Virology®

VACCINES AND ANTIVIRAL AGENTS

The High Content of Fructose in Human Semen Competitively Inhibits Broad and Potent Antivirals That Target High-Mannose Glycans

Jacklyn Johnson,[a] Manuel G. Flores,[a] John Rosa,[a] Changze Han,[a] Alicia M. Salvi,[b] Kris A. DeMali,[b] Jennifer R. Jagnow,[c] Amy Sparks,[c] Hillel Haim[a]

[a]Department of Microbiology and Immunology, Carver College of Medicine, University of Iowa, Iowa City, Iowa, USA
[b]Department of Biochemistry, Carver College of Medicine, University of Iowa, Iowa City, Iowa, USA
[c]In Vitro Fertilization and Reproductive Testing Laboratory, University of Iowa Hospitals and Clinics, Iowa City, Iowa, USA

ABSTRACT Semen is the primary transmission vehicle for various pathogenic viruses. Initial steps of transmission, including cell attachment and entry, likely occur in the presence of semen. However, the unstable nature of human seminal plasma and its toxic effects on cells in culture limit the ability to study *in vitro* virus infection and inhibition in this medium. We found that whole semen significantly reduces the potency of antibodies and microbicides that target glycans on the envelope glycoproteins (Envs) of HIV-1. The extraordinarily high concentration of the monosaccharide fructose in semen contributes significantly to the effect by competitively inhibiting the binding of ligands to α1,2-linked mannose residues on Env. Infection and inhibition in whole human seminal plasma are accurately mimicked by a stable synthetic simulant of seminal fluid that we formulated. Our findings indicate that, in addition to the protein content of biological secretions, their small-solute composition impacts the potency of antiviral microbicides and mucosal antibodies.

IMPORTANCE Biological secretions allow viruses to spread between individuals. Each type of secretion has a unique composition of proteins, salts, and sugars, which can affect the infectivity potential of the virus and inhibition of this process. Here, we describe HIV-1 infection and inhibition in whole human seminal plasma and a synthetic simulant that we formulated. We discovered that the sugar fructose in semen decreases the activity of a broad and potent class of antiviral agents that target mannose sugars on the envelope protein of HIV-1. This effect of semen fructose likely reduces the efficacy of such inhibitors to prevent the sexual transmission of HIV-1. Our findings suggest that the preclinical evaluation of microbicides and vaccine-elicited antibodies will be improved by their *in vitro* assessment in synthetic formulations that simulate the effects of semen on HIV-1 infection and inhibition.

KEYWORDS antibodies, HIV-1, high-mannose glycans, human semen, lectins, microbicides, seminal plasma simulant, sexual transmission

The envelope glycoproteins (Envs) on the surface of human immunodeficiency virus type 1 (HIV-1) are primary targets in the design of vaccines and microbicides. Env is a trimer composed of three gp120 surface subunits and three gp41 transmembrane subunits. The gp120 subunit is heavily glycosylated. Many of these glycans belong to the high-mannose class (1, 2), which contains 5 to 9 mannose residues attached to the *N*-acetylglucosamine core. Mannose residues are associated by several types of linkages, designated by the positions of the carbon atoms involved. High-mannose glycans most commonly contain α1,2-linked mannose residues (Manα1,2Man). These glycans

Citation Johnson J, Flores MG, Rosa J, Han C, Salvi AM, DeMali KA, Jagnow JR, Sparks A, Haim H. 2020. The high content of fructose in human semen competitively inhibits broad and potent antivirals that target high-mannose glycans. J Virol 94:e01749-19. https://doi.org/10.1128/JVI.01749-19.

Editor Frank Kirchhoff, Ulm University Medical Center

Address correspondence to Hillel Haim, Hillel-haim@uiowa.edu.

Received 11 October 2019
Accepted 17 February 2020
Accepted manuscript posted online 26 February 2020
Published 16 April 2020

are required for Env function and shield conserved epitopes from antibody recognition (3–6). Env glycans also serve as targets for broad and potent inhibitors of HIV-1 (7–9). For example, the monoclonal antibody (MAb) 2G12 targets an epitope composed of terminal Manα1,2Man residues (10–12). Other broadly neutralizing antibodies (BNAbs) can bind Env through dual protein-glycan epitopes (13–16). Such glycan-targeting antibodies have demonstrated potent antiviral activity *in vivo*, rendering their epitopes attractive targets in vaccine design (8, 17). Glycans on the surface of HIV-1 Env and other enveloped viruses are also recognized by carbohydrate-binding proteins designated lectins, which have been purified from diverse organisms (9, 18). Griffithsin (GRFT) is an alga-derived lectin that targets Manα1,2Man residues. This lectin potently inhibits infection by several sexually transmitted viruses, including HIV-1, herpes simplex virus type 2, and human papillomavirus (HPV) (9, 19). GRFT was shown to effectively prevent the vaginal transmission of these viruses in different animal models (20). A vaginal gel that contains GRFT is now being tested in a phase I clinical trial as an HIV-1 microbicide.

Semen is the primary vehicle for HIV-1 transmission (21). After vaginal intercourse, the ejaculate is the dominant medium in the female reproductive tract (the average volume is 7-fold greater than that of vaginal fluid) (22, 23). Over the course of several hours, the ejaculate is replaced by acidic vaginal secretions, which effectively inactivate the virus (24–27). Therefore, initial steps of infection (i.e., attachment of the virus to host cells and entry) likely occur in the presence of semen. Accordingly, potential microbicides and vaccine-elicited antibodies must be effective in this medium. Several studies have examined the effects of semen on virus infection and inhibition. Due to the unstable nature and cytotoxicity of seminal fluid (28–31), these studies were performed using (i) diluted samples, (ii) purified semen components, or (iii) protocols that expose only virus and not cells to undiluted semen (28, 29, 32–36). Such experimental designs limit our ability to evaluate the effects of semen on the entire entry process and on virus inhibition under the conditions that may occur during sexual transmission of the virus.

Semen is unique among body fluids for a high concentration of the monosaccharide fructose (average, 15 mM; normal range, 5 to 30 mM) (22), which is required to support sperm viability, function, and motility. Such levels are more than 3-fold higher than those of glucose in semen and more than 300-fold higher than those of fructose in blood. Consequently, during vaginal transmission, viruses from the infected partner encounter recipient host cells and inhibitory agents in the presence of fructose. Since glycan-targeting antivirals can bind soluble sugars (12, 19, 37, 38), we hypothesized that the potency of these agents may be reduced by the high content of fructose in human semen. Indeed, fructose significantly reduced the inhibition of HIV-1 by agents that target glycans containing terminal Manα1,2Man residues. In whole and fractionated seminal plasma (SP), fructose levels varied between donors. Inhibition of HIV-1 by the lectin GRFT in these samples was greatly reduced and correlated with the concentration of fructose in each.

RESULTS

Fructose reduces binding and inhibition of HIV-1 by the glycan-targeting antibody 2G12. We hypothesized that the high content of fructose in semen may affect HIV-1 inhibition by glycan-targeting inhibitors. To test this hypothesis, we examined the effects of different monosaccharides on the binding of MAb 2G12, which targets a glycan-dependent epitope on Env composed of Manα1,2Man residues (10, 11). Full-length HIV-1 Envs from diverse transmitted/founder (T/F) strains or from chronically infected patients were expressed on the surface of human osteosarcoma (HOS) cells. These cells efficiently process Env into gp120 and gp41 subunits (39). Env-expressing cells were incubated with MAb 2G12 in Dulbecco's modified Eagle medium (DMEM) supplemented with glucose, mannose, or fructose. Binding of the MAb was measured by a cell-based enzyme-linked immunosorbent assay (ELISA) (Fig. 1A). Consistent with previous reports (12), glucose did not reduce (or even modestly

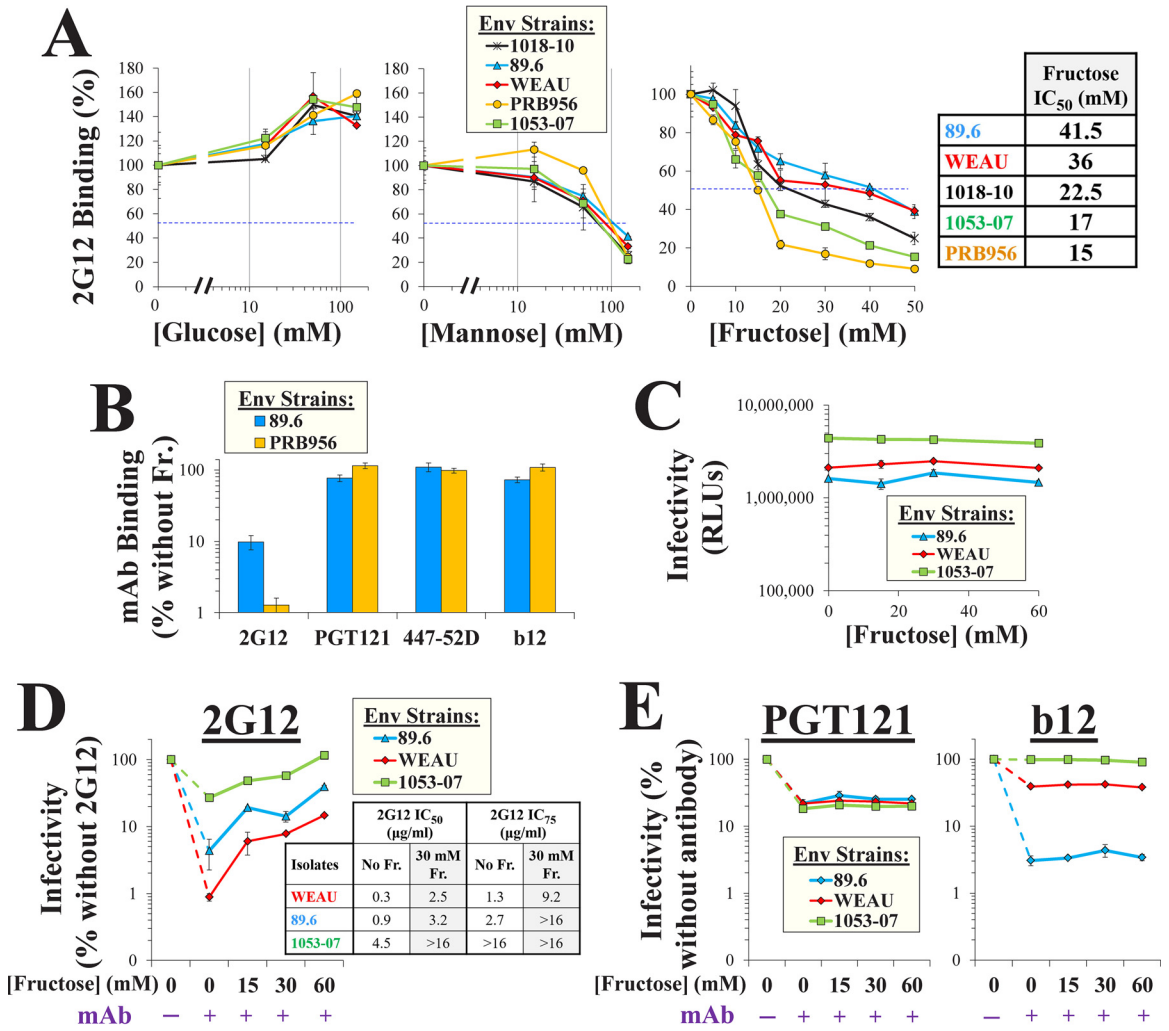

FIG 1 Fructose reduces the binding and inhibition of HIV-1 by the glycan-targeting MAb 2G12. (A) Binding of MAb 2G12 to Env in the presence of different monosaccharides. Full-length Envs of diverse HIV-1 strains were expressed on HOS cells. Samples were incubated for 45 min with MAb 2G12 (2 μg/ml) in DMEM supplemented with glucose, mannose, or fructose, and binding was measured by a cell-based ELISA. Values describe 2G12 binding as a percentage of that measured without saccharide. (Inset) The fructose concentrations that reduced binding by 50% (IC_{50}) are indicated. Error bars, standard errors of the means (SEM) from two replicates. Results are representative of those from two independent experiments. (B) Effects of fructose (Fr.; 150 mM in DMEM) on binding of MAbs to Envs of strains 89.6 and PRB956 expressed on cells. (C) Effects of fructose on HIV-1 infection. Luciferase-expressing viruses containing the indicated Envs were incubated for 1 h at 37°C in DMEM supplemented with the indicated concentrations of fructose. Samples were then added to Cf2Th $CD4^+$ $CCR5^+$ cells, and residual infectivity was measured 72 h later. Luciferase activity is shown in relative light units (RLUs). (D, E) HIV-1 neutralization by MAbs in the presence of fructose. Viruses were incubated in DMEM supplemented with fructose and MAb 2G12 (15 μg/ml), PGT121 (3 μg/ml), or b12 (4 μg/ml) and then added to target cells. Infection is expressed as a percentage of the level of infection without MAb (shown in panel C). (Inset in panel D) The concentrations of MAb 2G12 required to reduce infectivity by 50% and 75% in the absence or presence of fructose are shown. Error bars, SEM.

increased) the binding of 2G12 to the Envs. High levels of mannose inhibited 2G12 binding; the concentrations required for a 2-fold reduction (the 50% inhibitory concentration [IC_{50}]) ranged from 80 to 120 mM. Fructose inhibited 2G12 binding more efficiently than mannose; IC_{50} values ranged from 15 to 41.5 mM (Fig. 1A, inset). Such concentrations are mostly within the normal range for human semen (22). The fructose-mediated effect on 2G12 binding was inversely related to the efficiency of the interaction with each Env; strains that bound 2G12 more effectively were less affected by fructose ($P = 0.003$ in a Spearman correlation test). Binding of the dual glycan-protein-targeting MAb PGT121, which can recognize high-mannose glycans on viruses and isolated Envs (13, 15, 16), was unaffected by fructose, even at 150 mM of the saccharide (Fig. 1B). Similarly, fructose did not alter the binding of MAbs 447-52D and b12, which

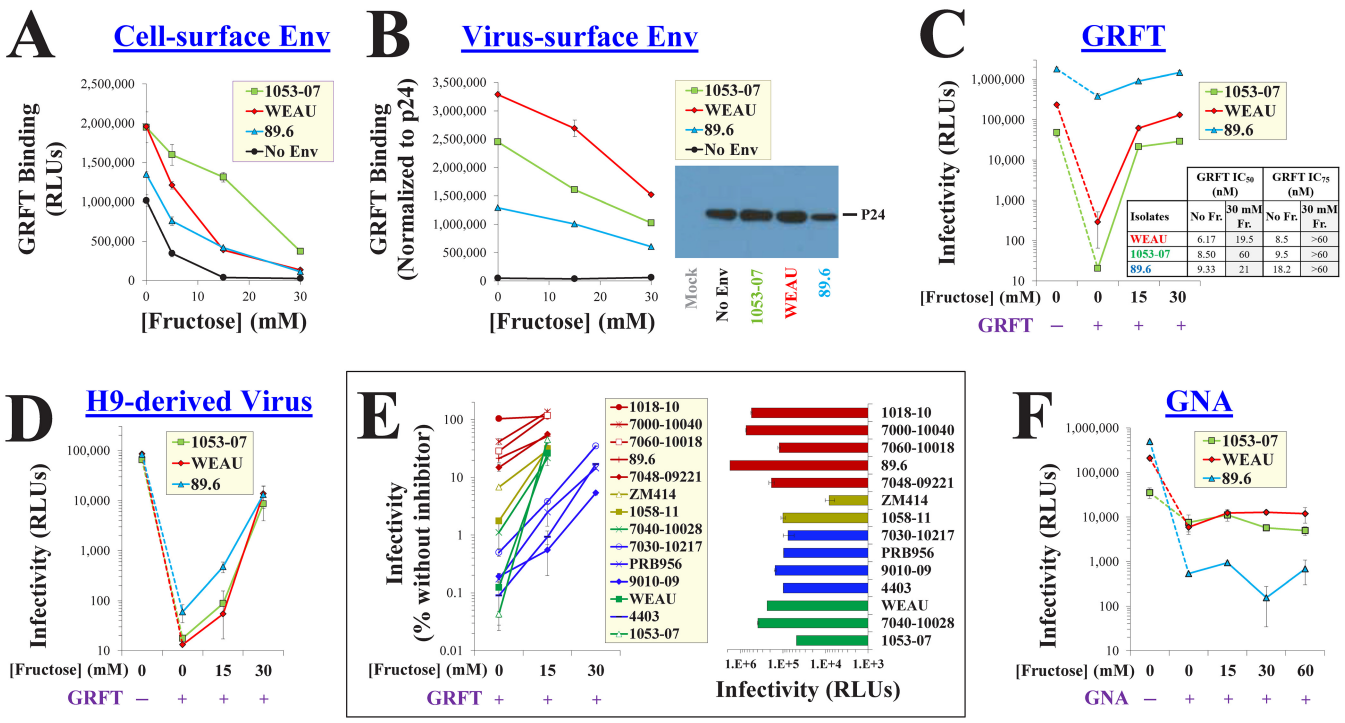

FIG 2 Fructose reduces the binding efficiency and inhibitory potency of the lectin microbicide GRFT. (A) Binding of GRFT to Envs expressed on HOS cells in the presence of fructose. His-tagged GRFT was incubated with Env-expressing HOS cells in DMEM supplemented with different concentrations of fructose. The cells were then washed, and GRFT binding was measured using an anti-His antibody suspended in fructose-free buffer. To quantify Env-independent binding, cells were transfected with a plasmid containing a premature stop codon in the *env* gene (labeled "No Env"). (B) GRFT binding to Env on virus particles. Virus stocks that contained the indicated Envs (or no Env) were produced in 293T cells and attached to protein-binding plates. (Left) GRFT binding was measured by ELISA in DMEM containing the indicated fructose concentrations. (Right) Each virus stock was also analyzed by SDS-PAGE to quantify the virus capsid (p24 antigen) content. GRFT binding values were normalized to the amount of p24 in each sample. (C) Effects of fructose on HIV-1 inhibition by GRFT. Viruses produced in 293T cells were incubated with target cells in DMEM supplemented with fructose in the absence or presence of 30 nM GRFT. (Inset) IC_{50} and IC_{75} values for GRFT in the different media are shown. (D) Effects of fructose on GRFT inhibition of viruses produced in H9 cells. (E) (Left) Fructose rescue of infection by diverse HIV-1 strains in the presence of GRFT. (Right) Infection by each strain in the absence of GRFT. HIV-1 strains are color coded by GRFT sensitivity (red, resistant; yellow, intermediate; green and blue, sensitive) and by the concentration of fructose required to abrogate GRFT inhibition (green, 15 mM; blue, 30 mM). (F) Effects of fructose on inhibition of virus infectivity by GNA (400 nM).

target glycan-independent epitopes on the V3 loop and the CD4-binding site of Env, respectively (Fig. 1B).

We examined whether the fructose-mediated decrease in 2G12 binding reduced the neutralizing potency of this antibody. Luciferase-expressing viruses were incubated with MAbs in the absence or presence of fructose and added to *Canis familiaris* thymus normal (Cf2Th) cells, which express CD4 and CCR5, to measure infection. Fructose did not affect virus infectivity (Fig. 1C). Antibody 2G12 neutralized viruses containing the diverse Envs by 4- to 100-fold (Fig. 1D). In the presence of 2G12, fructose rescued infectivity in a concentration-dependent manner: at 30 mM, infection was increased by up to 10-fold (see the IC_{50} and IC_{75} values of 2G12 in the inset of Fig. 1D). By comparison, fructose did not rescue infection in the presence of MAb PGT121 or b12 (Fig. 1E). Therefore, the concentrations of fructose normally found in semen reduce the binding and potency of the glycan-targeting MAb 2G12.

Fructose reduces binding and inhibition of HIV-1 by the lectin microbicide griffithsin. The lectin griffithsin (GRFT) is a broad and potent inhibitor of HIV-1 (40). Each subunit of this homodimer contains three carbohydrate-binding pockets, which recognize terminal Manα1,2Man residues on Env (11, 41). We examined whether the binding of GRFT to Envs expressed on the surface of cells is affected by fructose. In the absence of Env, the His-tagged GRFT bound to the cells (Fig. 2A), likely reflecting recognition of cell-surface glycans (42). Expression of Env on the cell surface enhanced binding by 1.5- to 2-fold. In the presence of 15 mM fructose, GRFT binding to Env-negative cells was lost, whereas binding to Env-expressing cells was decreased but not

abrogated. We also examined the effect of fructose on GRFT binding to Envs on the surface of virus particles. Viruses were attached to protein-binding plates. GRFT binding was then measured by ELISA and normalized for the virus particle content in each sample by the p24 antigen content. In contrast to cell-based measurements, the binding of GRFT to viruses was strictly Env dependent; negligible binding to particles that lacked Env was detected (Fig. 2B). Addition of fructose modestly reduced the binding of GRFT to the virus-surface Envs. Since modest changes in binding can significantly impact the potency of GRFT (43, 44), we examined the effects of fructose on GRFT inhibition. As expected, sensitivity to GRFT varied between the diverse Envs (41, 45); 30 nM of this lectin inhibited infection between 5- and 2,000-fold (Fig. 2C). Importantly, fructose at the concentrations found in semen (15 to 30 mM) increased GRFT IC_{50} and IC_{75} values significantly (Fig. 2C, inset).

Viruses produced in different cell types can exhibit distinct patterns of glycosylation (46, 47). We compared the GRFT sensitivity of viruses produced in 293T cells (Fig. 2C) and in the human T-lymphocyte cell line H9 (Fig. 2D). H9-derived viruses that contained 1053-07 and WEAU Envs were as sensitive to GRFT as the same viruses produced in 293T cells. However, H9-derived virus that contained the 89.6 Env was significantly more sensitive to GRFT than virus from 293T cells. Fructose rescue of infection by H9-derived viruses was most pronounced at concentrations between 15 and 30 mM (relative to a concentration of 15 mM in 293T-derived viruses). Therefore, viruses produced in the two cell types can vary in sensitivity to GRFT; nonetheless, the concentrations of fructose normally found in semen rescued the infectivity of both.

To determine the breadth of the fructose-mediated rescue of infectivity, we expanded the Env panel to include Envs from 15 clade B and C strains. The effects of fructose on GRFT inhibition varied between strains (Fig. 2E). For example, strain WEAU and 4403 Envs were similarly sensitive to GRFT; however, fructose at 15 mM rescued the infection of strain WEAU more than 200-fold but minimally affected strain 4403 (the latter required 30 mM to rescue infectivity to the same extent as that of WEAU). Sensitivity of the strains to fructose rescue of infection (Fig. 2E, left) and their infectivity in the absence of fructose (Fig. 2E, right) were not associated.

We examined whether fructose affects a second lectin inhibitor of HIV-1. *Galanthus nivalis* agglutinin (GNA) is a plant-derived lectin that targets terminal α1,3- and α1,6-linked mannose residues (45, 48). As expected, the sensitivity of the Envs to GNA did not correspond with their sensitivity to GRFT (48) (compare Fig. 2C and F). Interestingly, in contrast to GRFT, which targets Manα1,2Man residues, GNA inhibition was unaffected by fructose, even at very high concentrations of the saccharide (Fig. 2F).

These results suggest that the effects of fructose are specific for Manα1,2Man-targeting agents. As previously shown, the distribution of such moieties varies between virus strains and producer cell types (1, 46). Accordingly, the sensitivity of each Env to GRFT cannot be fully explained by the presence of potential N-linked glycosylation sites (PNGSs) at specific positions of Env (41, 45, 49) (see the PNGS occupancy of all Envs tested in Data Set S1 in the supplemental material). The differential effects of fructose on the diverse isolates likely reflect the efficiency of GRFT binding to each Env, which is determined by the distribution of the Manα1,2Man residues. The concentrations of fructose normally found in semen competitively inhibited this interaction and rescued HIV-1 infectivity in a broad and effective manner.

The potency of inhibitors that target Manα1,2Man residues is reduced by fructose in a simulant of hSP. To investigate the effects of fructose on HIV-1 inhibitors in a medium with a chemical composition similar to that of human seminal plasma (hSP), we generated a simulant of SP (sSP). The composition of the simulant was modified from the commonly applied formulation developed by Owen and Katz (22, 50) to better reflect the ionic content of semen and to increase stability (Table 1). Relative to the above-mentioned formulation, the modified simulant does not precipitate at 37°C (Fig. 3A). Furthermore, in contrast to hSP, which rapidly reduces the viability of cells in culture (28, 51), the sSP formulation is nontoxic over a 5-h incubation period (Fig. 3B). Since hSP samples were also analyzed in this study, we sought to establish a

TABLE 1 Solute composition of human seminal plasma and the simulant used in this study

Solute	Concn[a] (mM) in:	
	Human seminal plasma	Simulant of seminal plasma
Sodium	130.4	117.8
Chloride	40	39.2
Potassium	27.9	27.9
Calcium	6.9	7
Magnesium	4.5	4.5
Zinc	2.5	2
Phosphate	7.8	7.8
Bicarbonate	20	20
Lactic acid	6.9	7
Citrate	27.5	27.6
Urea	7.5	7.5
Fructose	15.1	*[b]
Glucose	5.7	6
Albumin	0.23	0.76
Total protein	0.76	0.76
pH	7.7	7.7
Buffering capacity[c]	25	18.3

[a]The values are the average concentrations of the major solutes in hSP, based on a literature review (22), unless indicated otherwise.
[b]*, concentration, as indicated throughout the text.
[c]Buffering capacity is given in slykes. The normal range for human semen is 15 to 40 slykes.

protocol that would allow the entire fusion process to occur in whole semen with limited induction of cell death. The protocol is outlined in Fig. 3C. Virus particles are attached to protein-binding plates and then exposed to 97.5% sSP or hSP in the absence or presence of inhibitors. Cells are then added to the samples (final concentration of SP, 77.5%) and infection is allowed to proceed for 75 min. The infection medium is then removed, and cells are trypsinized to detach bound virions and further incubated for 3 days with the fusion inhibitor enfuvirtide (T-20) to prevent further entry. The infectivity of viruses containing the WEAU and 1053-07 Envs was reduced in sSP relative to that measured in DMEM by 2- and 6-fold, respectively (Fig. 3D). Measurements of virus entry after longer incubation periods showed conserved 2-fold differences between sSP and DMEM for both strains (Fig. 3E). Such modest differences did not result from the effects of sSP on cell viability (Fig. 3F). Furthermore, sSP did not cause greater detachment of cells from the culture plates (Fig. 3G). To increase the sensitivity of viability measurements, we examined whether a 75-min exposure to sSP (without or with fructose) was associated with the induction of cellular apoptosis by annexin V staining. No significant increase in the proportion of apoptotic cells was observed in the samples incubated with the sSPs relative to that in the samples incubated with DMEM (Fig. 3H).

Therefore, the simulant of human seminal plasma does not reduce the viability of cells relative to their viability in DMEM. We attributed the 2-fold lower infectivity in sSPs (relative to that in DMEM) to differences in the solute composition of the media, primarily to pH (pH 7.7 in sSP relative to pH 7.4 in DMEM). Analysis of a panel of 11 T/F Envs from clades B and C showed that such an increase in pH reduces infectivity by an average of 1.6-fold (data not shown). In addition, the 10% fetal calf serum (FCS) used to supplement DMEM can increase HIV-1 infection by up to 2-fold (52). Other solutes found in human semen (including urea, high levels of calcium and magnesium, lactic acid, and citric acid) may alter infectivity in a strain-specific manner and explain the modestly lower entry rate of isolate 1053 relative to that of isolate WEAU (27, 53, 54).

We examined the effects of sSP on HIV-1 inhibition by different agents (Fig. 4A). For both viruses tested, inhibition was similar in DMEM and fructose-free sSP [sSP(−Fr)]. Addition of fructose to sSP rescued virus infectivity in the presence of GRFT. Relatively modest effects of fructose were observed on MAb 2G12, which showed a 2-fold rescue

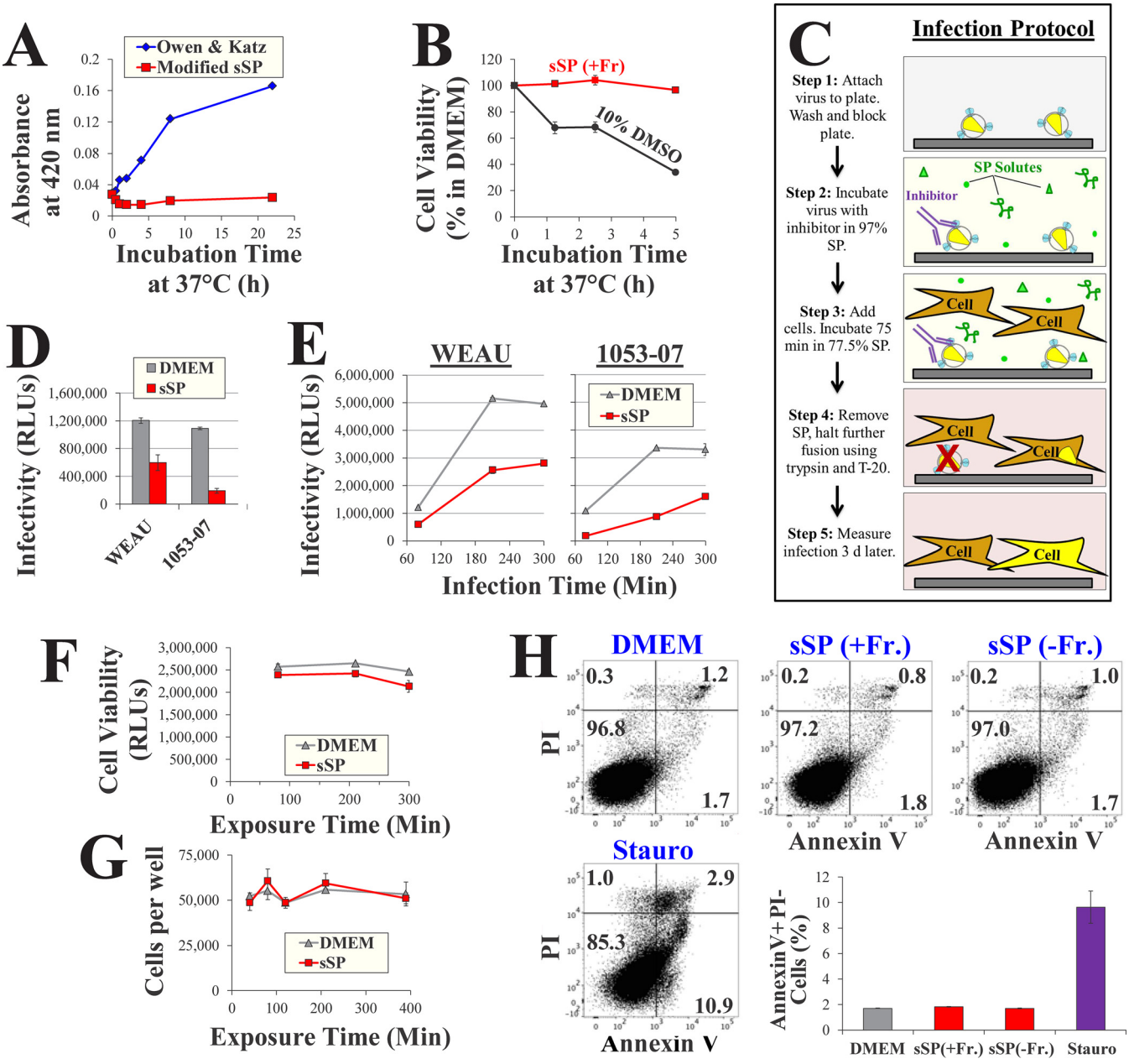

FIG 3 HIV-1 infectivity and cell viability in a simulant of seminal plasma. (A) Precipitation in simulants of seminal plasma. Simulants were incubated at 37°C for different time periods, and precipitation was measured by determination of the absorbance at 420 nm. (B) Cell viability in sSP. Cf2Th CD4$^+$ CCR5$^+$ cells were incubated in sSP supplemented with 15 mM fructose [sSP(+Fr)] at 37°C for different time periods, washed, and further cultured in DMEM for 36 h. Cell viability was measured by an ATP-based assay. Samples exposed to the cytotoxic agent dimethyl sulfoxide (DMSO) were tested as a control. (C) Schematic of virus infectivity tests in SP. d, days. (D) Infection measured by the protocol outlined in panel C for viruses containing the indicated Envs. (E) Rate of HIV-1 entry in sSP. Cells were incubated with viruses in sSP or DMEM for different time periods before infection was halted by trypsin and T-20 (step 4). (F) Viability in samples treated as described in the legend to panel E was measured after 36 h. (G) Samples were treated as described in panel C in DMEM or sSP(+Fr) (15 mM) for the indicated times. The cells were then washed three times, detached with trypsin-EDTA, and counted. (H) Apoptosis induction by DMEM and sSP. Cf2Th cells were incubated with DMEM, sSP containing 0 or 15 mM fructose, or DMEM supplemented with 4 μM the apoptosis-inducing agent staurosporine (Stauro) for 75 min at 37°C. The cells were then washed, further incubated in DMEM for 14 h, stained by annexin V and propidium iodide (PI), and analyzed by flow cytometry. Mean values for annexin V-positive, propidium iodide-negative cells in two replicate samples are shown. Error bars, SE.

for both Envs. The effects of fructose on GNA and MAbs PGT121 and b12 were not significant. The fructose-mediated rescue of infection in the presence of GRFT was concentration dependent; at 30 mM, fructose increased infection more than 175-fold (Fig. 4B, top). More modest effects of fructose were observed in the presence of MAb 2G12; at 30 mM, infection was rescued by up to 2.5-fold. Similar fructose-mediated

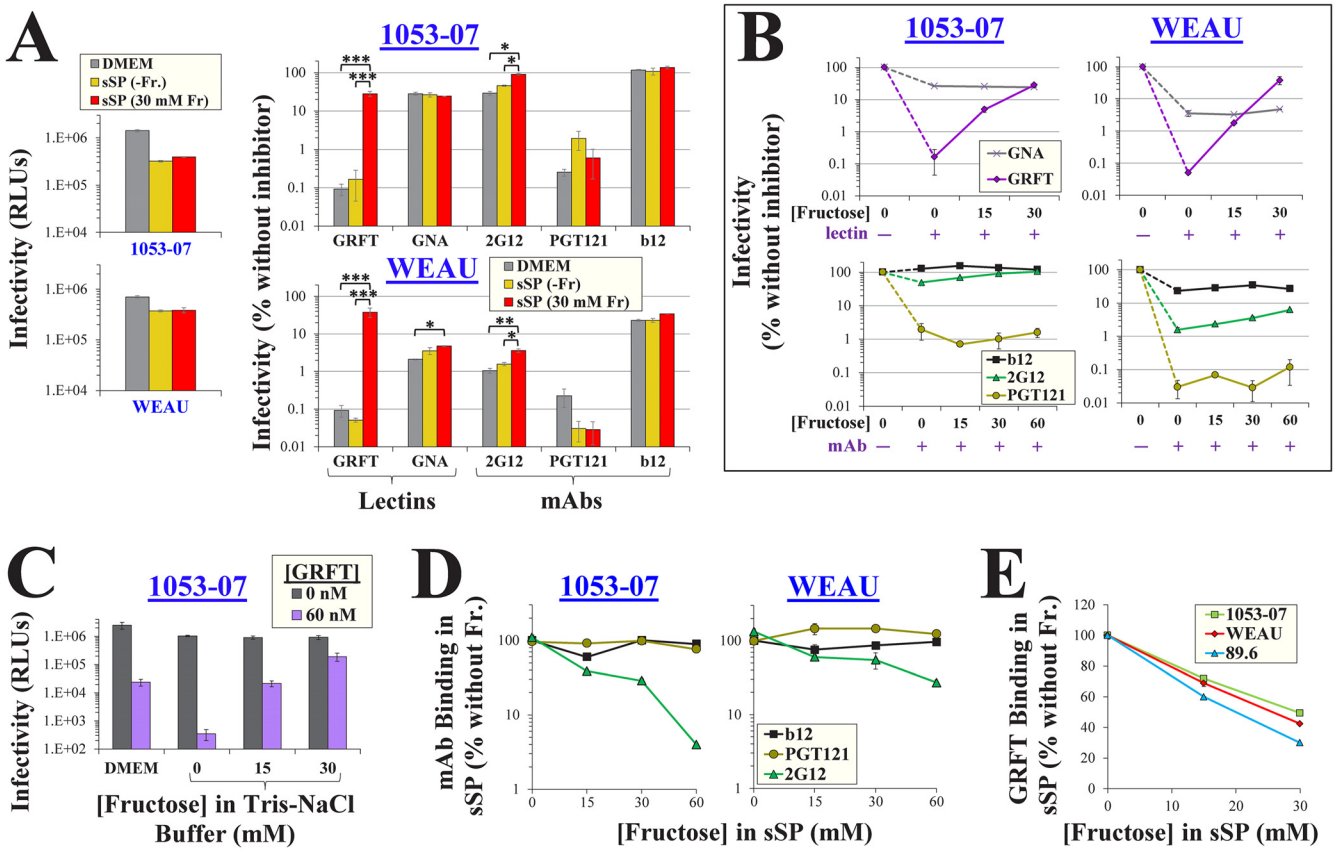

FIG 4 Fructose reduces the potency of GRFT and MAb 2G12 in a simulant of seminal plasma. (A) Effects of fructose on HIV-1 inhibition by lectins and MAbs. Infection by viruses containing strain 1053-07 or WEAU Envs was measured in DMEM, sSP(−Fr), or sSP containing 30 mM fructose using the protocol outlined in Fig. 3C. Infection was also measured in the presence of GRFT (60 nM), GNA (400 nM), MAb 2G12 (15 μg/ml), MAb PGT121 (3 μg/ml), or MAb b12 (10 μg/ml). Infection in the presence of each inhibitor is expressed as a percentage of the level of infection measured in the absence of inhibitors. Error bars, SEM. *P* values were determined by a two-tailed *t* test. *, $P < 0.05$; **, $P < 0.005$; ***, $P < 0.0005$. (B) Effects of fructose on inhibition of virus infection in sSP. (C) Effects of fructose on inhibition of virus infection in Tris-buffered saline (150 mM NaCl, 20 mM Tris base, pH 7.5). (D) Binding of antibodies to Envs in sSP. The indicated MAbs (all at 0.5 μg/ml) were suspended in sSP containing different concentrations of fructose, and the media were incubated with HOS cells that expressed 1053-07 or WEAU Envs. Values are expressed as a percentage of the level of binding in the absence of fructose. (E) GRFT binding to HIV-1 in sSP. The binding of His-tagged GRFT to virus particles that contained the indicated Envs was measured in the presence of different fructose concentrations and is expressed as a percentage of the level of binding in the absence of fructose. Error bars, SEM.

effects on GRFT were observed in a Tris-NaCl buffer (Fig. 4C). In comparison, the inhibitor GNA and MAb PGT121 were unaffected by fructose (Fig. 4B). The effects of fructose on virus inhibition by the different agents corresponded with its effects on inhibitor binding (Fig. 4D and E); addition of this saccharide to sSP reduced the binding of 2G12 and GRFT, whereas the binding of PGT121 and b12 was unaffected.

Therefore, in a simulant of seminal plasma, fructose reduces HIV-1 binding and inhibition by agents that target Manα1,2Man residues. The lectin inhibitor GRFT is highly sensitive to the fructose-mediated effects, whereas MAb 2G12 is more modestly affected.

Seminal plasma from human donors exhibit a range of fructose concentrations and exert different effects on the potency of HIV-1 inhibitors. We examined the effects of semen samples from human donors on HIV-1 inhibition and the relationship with their fructose content. Whole hSP samples were obtained from HIV-negative donors that visited the In Vitro Fertilization and Reproductive Testing Laboratory at the University of Iowa Hospitals and Clinics. The effects of the hSP samples on cell viability were measured (Fig. 5A). For most donor samples tested, cell viability was minimally affected after a 75-min exposure. As expected, longer exposure times caused a gradual decrease in cell viability (51). This window of viability (75 min) is sufficient to analyze HIV-1 infection and inhibition (Fig. 3C and D and Fig. 4A).

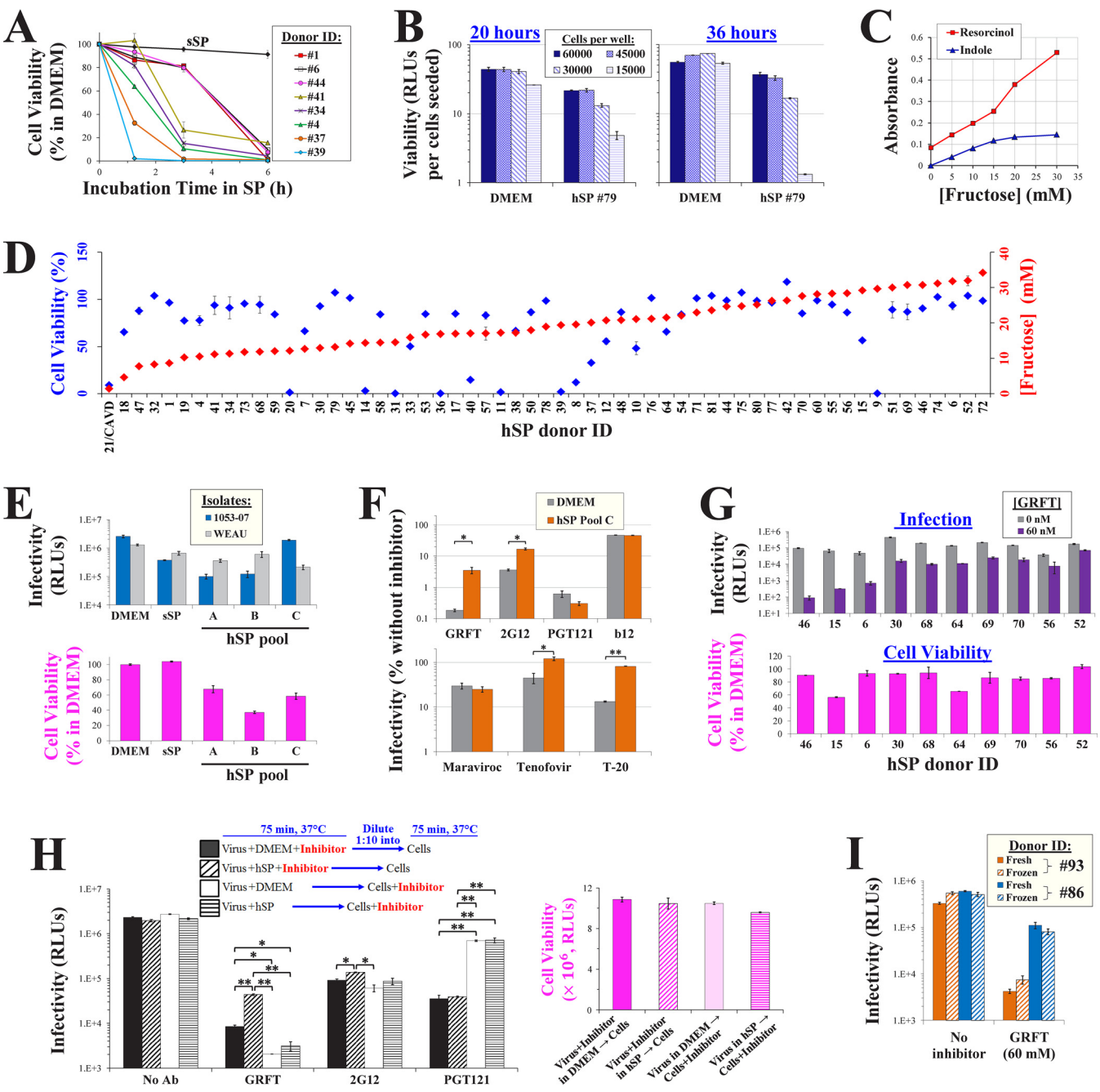

FIG 5 HIV-1 infection and inhibition in human seminal plasma. (A) Dynamics of SP cytotoxicity. Cf2Th CD4$^+$ CCR5$^+$ cells were incubated with whole hSP from different donors or with sSP(+Fr) for the indicated times, washed, and cultured in DMEM for 36 h. Cell viability was measured by an ATP-based assay. (B) Cf2Th CD4$^+$ CCR5$^+$ cells were added to 96-well plates at the indicated densities. Samples were then incubated at 37°C for 75 min with DMEM or a sample containing 77.5% hSP and 22.5% Tris-saline buffer. All samples were then washed and further processed as described in Fig. 3C, and viability was measured after 20 or 36 h. Viability values are corrected for the number of cells seeded in each well. (C) Fructose concentrations measured by the resorcinol and indole assays. Fructose standards were diluted in Tris-buffered saline (pH 7.5). (D) Cell viability (after 75 min of exposure) and fructose content (quantified by resorcinol) in 59 hSP samples from different donors were measured. Since samples were tested in separate experiments, values are reported as a percentage of the viability in the DMEM control included in each assay. CAVD, congenital absence of the vas deferens. (E) Infection by virus containing strain 1053-07 or WEAU Envs in DMEM, sSP(+Fr), and three pools of donor hSP using the protocol shown in Fig. 3C. Cell viability was measured in the same experiment. (F) HIV-1 inhibition in hSP. Infection by virus that contains the WEAU Env was measured in DMEM and whole pooled hSP from 10 donors (pool C) in the presence of GRFT (60 nM), 2G12 (20 μg/ml), PGT121 (3 μg/ml), b12 (15 μg/ml), maraviroc (1 μM), tenofovir (2 μM), or T-20 (6 μM). Cell viability after exposure to hSP pool C was measured in the same experiment and was 59.8% of that measured in DMEM. Error bars, SEM. *P* values were determined by a two-tailed *t* test. *, $P < 0.05$; **, $P < 0.005$. (G) GRFT inhibition of virus containing the 1053-07 Env in hSP samples from different donors. Viability values are expressed as a percentage of those measured in samples incubated with DMEM. (H) (Left) Immobilized viruses containing the WEAU Env were treated as shown, using GRFT (50 nM), 2G12 (20 μg/ml), or PGT121 (3 μg/ml). Entry was then halted using trypsin and T-20, and infectivity was measured 3 days later. (Right) The viability of samples similarly treated in the same experiment was measured after 36 h. (I) Infection and GRFT inhibition in fresh and thawed hSPs. Samples were collected from donors and either subjected to one freeze-thaw cycle (frozen) or left at room temperature (fresh) for 4 h, before they were used for infection assays in the absence or presence of GRFT.

Human seminal plasma is toxic to cell cultures (28, 33, 36). Interestingly, recent reports have shown that it exerts limited toxic effects on colon and vaginal tissue explants (55, 56). We hypothesized that the high density of cells in the explants may explain the low toxicity. To test this possibility, we incubated Cf2Th $CD4^+$ $CCR5^+$ cells at different densities in 96-well plates and exposed them to DMEM or hSP for 75 min. The cells were then processed as described in Fig. 3C, and viability was measured after 20 or 36 h. We found that at both time points the lower-confluence samples exposed to hSP were significantly less viable than the higher-confluence samples (Fig. 5B). Viability in hSP-exposed samples containing 15,000 cells per well (approximately 70% confluence) was reduced 6-fold at 20 h and 41-fold at 36 h relative to viability in samples incubated with DMEM. By contrast, viability in hSP-exposed samples containing 60,000 cells per well was reduced 2.1-fold at 20 h and 1.5-fold at 36 h relative to viability in samples incubated with DMEM.

Clinical evaluation of human semen includes a qualitative analysis of fructose as an indicator of seminal vesicle function. Two standard assays, which use the colorimetric reagents resorcinol and indole, are commonly applied for this purpose (57, 58). We performed both assays to quantify fructose concentrations using a range of fructose standards (Fig. 5C). Only the resorcinol assay could accurately quantify fructose at concentrations higher than 15 mM. We used this assay to measure fructose in 59 donor samples (Fig. 5D). Consistent with previous reports (22), the fructose concentration ranged from 5 to 34 mM (average concentration, 18 mM). As a control, we used hSP from a donor with congenital absence of the vas deferens (CAVD). Since secretions from the seminal vesicles are blocked in such individuals, negligible levels of fructose were detected in the sample (59). We also measured the cytotoxicity induced by each hSP sample after a 75-min exposure to the cells (Fig. 5D). A wide range of viability levels was observed; 62% of samples exhibited viability at least 75% of that measured in DMEM-treated cells. No association was observed between the concentration of fructose in a sample and the toxicity that it induced ($P = 0.389$ in a Spearman correlation test).

We measured infectivity in sSP and in three samples of whole pooled hSP using viruses that contained the Envs of isolates 1053-07 and WEAU. As expected, infectivity in DMEM was higher than that in the sSP and hSP samples (Fig. 5E, top). Similar levels of viability were measured in DMEM and sSP, whereas viability was reduced in the hSP pools (Fig. 5E, bottom). Infectivity in sSP and the hSP pools was similar and did not correspond with sample viability. We examined the effects of whole hSP on inhibition of WEAU by different inhibitors. GRFT and MAb 2G12 were 25- and 5-fold less inhibitory in hSP than in DMEM, respectively (Fig. 5F, top). In comparison, inhibition by MAbs PGT121 and b12 was unaffected by hSP. As previously reported (36), inhibition by the CCR5 antagonist maraviroc was unaffected by hSP, whereas inhibition by the reverse transcriptase inhibitor tenofovir was reduced (Fig. 5F, bottom). Inhibition by the fusion inhibitor T-20, which targets a nonglycan motif in the heptad repeat region 1 of gp41 (60), was also reduced in whole hSP.

We asked whether the effects of hSP on virus inhibition differ between donor samples. To examine this, we measured GRFT inhibition of isolate 1053-07, which is highly sensitive to the effects of fructose (Fig. 5G). GRFT inhibition in the different donor samples ranged from 2.5-fold (in hSP from donor 52) and 1,000-fold (in hSP from donor 46). These differences did not correspond with virus infection in the absence of the inhibitor ($P = 0.230$ in a Spearman correlation test). Similarly, GRFT inhibition did not correspond with cell viability in each sample ($P = 0.312$ in a Spearman correlation test).

Human seminal plasma has previously been shown to reduce HIV-1 inhibition by a wide range of agents (36). In that study, virus was preincubated with hSP, followed by addition into a larger volume of medium containing the target cells and inhibitor. The authors discovered that complexes formed in semen by cationic peptides (designated semen enhancers of virus infection [SEVI]) increase the rate of virus attachment to cells, thus reducing the potency of inhibition. We performed neutralization assays using a similar dilution-based approach, which limits cell toxicity (33, 36). As described above, immobilized viruses were used in these experiments; these viruses rapidly interact with

the cells to initiate infection. Consequently, this approach eliminates SEVI-mediated effects on cell attachment and allows us to focus on the effects of semen on the virus-inhibitor interaction. The experimental design is schematically described in Fig. 5H. Two approaches were used. In the first, the virus was preincubated with hSP or DMEM in the presence of inhibitor and then diluted 1:10 by DMEM that contained the target cells. In the second, virus was preincubated with hSP or DMEM, followed by a 1:10 dilution into medium that contained cells and inhibitor. We found that preincubation of virus with GRFT in hSP rescued infection by 5.2-fold relative to that measured after preincubation with GRFT in DMEM (Fig. 5H). By comparison, for a similar level of inhibition, the protocol that incubated virus, cells, and inhibitor in 77.5% hSP showed a 17.5-fold rescue of infection relative to DMEM (Fig. 5F). No significant rescue of infection was observed when virus was preincubated with hSP and then diluted by GRFT-containing DMEM with cells. Preincubation with 2G12 showed a modest 1.5-fold rescue by hSP relative to DMEM (compared with 4.6-fold in Fig. 5F). When 2G12 was suspended in the cell-containing medium, no difference was observed between samples preincubated in hSP and DMEM. Consistent with the data in Fig. 5F, similar inhibition was observed for PGT121 in DMEM and hSP. Interestingly, samples preincubated with PGT121 (in hSP or DMEM) showed ~20-fold greater inhibition than samples in which antibody exposure occurred with the cells. We believe that this distinct pattern results from the different time frames for inhibition by the agents (61). PGT121 inactivates Env by binding to the native (unliganded) Env and inducing conformational changes in the CD4-binding site (16). In contrast, 2G12 (and, likely, GRFT) can interact with the virus after binding of CD4 (61). Therefore, when CD4 engagement occurs rapidly, the window of opportunity for PGT121 inhibition is reduced relative to that for 2G12 inhibition (and, likely, relative to that for GRFT inhibition), whereas preincubation of the virus with PGT121 before addition to cells allows effective neutralization. In summary, under dilution-based conditions that reduce cell toxicity, we still observed an hSP-mediated reduction of GRFT potency, whereas a modest reduction was observed for 2G12. Such effects are less pronounced than those detected using the protocol that allows both inhibition and entry to occur in minimally diluted hSP (Fig. 5F).

Finally, since the hSP samples were stored at −80°C before use, we examined whether a freeze-thaw cycle could alter their effects on inhibitor potency. Fresh seminal plasma samples from donors 86 and 93 were either frozen and thawed or directly tested for their effects on infection and GRFT inhibition. Both virus infectivity and virus inhibition were unaltered by the freeze-thaw cycle (Fig. 5I).

Therefore, antibodies and HIV-1 inhibitors are differentially affected by human seminal plasma. The effects on the lectin microbicide GRFT were the most notable. Toxic effects of hSP on the cells could potentially reduce infection and thus present a spurious pattern of altered inhibitor potency. Several lines of evidence suggest that the patterns of inhibition are not related to sample toxicity: (i) SP effects are inhibitor specific, as the potency of some agents (e.g., GRFT, T-20, and tenofovir) is reduced by sSP and hSP, whereas that of other agents (e.g., maraviroc and PGT121) is unaffected; (ii) after a 75-min incubation period in hSP, cell viability was not associated with the measured level of infectivity or inhibition; and (iii) the SP simulant, which showed levels of viability and apoptosis induction identical to those for DMEM, exhibited the same patterns of infectivity and inhibition as hSP, which differed significantly from the patterns observed for DMEM.

Both small- and large-solute fractions of human seminal plasma reduce the potency of glycan-targeting inhibitors. Different proteins and molecular complexes isolated from semen can affect HIV-1 entry and inhibition (36, 62–64). To differentiate between the effects of such large solutes and those of the small solutes (e.g., salts and saccharides), we fractionated hSP samples using filters with a 3-kDa-molecular-weight cutoff (MWCO) (Fig. 6A). The filtrate, containing small hSP solutes, was collected. The retained fraction, which contained solutes larger than 3 kDa, underwent buffer exchange to replace the small solutes with those of sSP(−Fr). As expected, the concen-

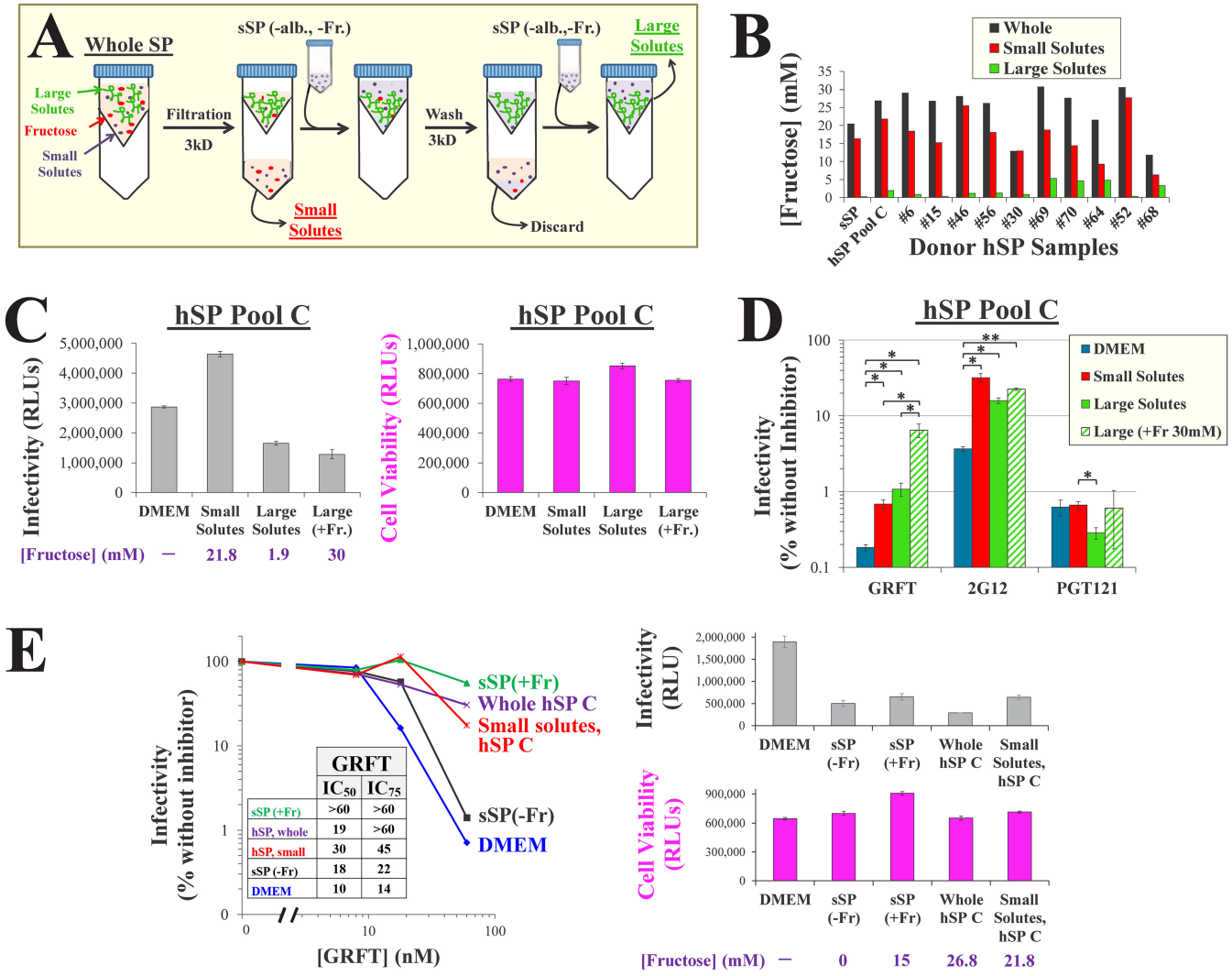

FIG 6 The small and large solutes of human seminal plasma reduce the potency of HIV-1 inhibitors. (A) Separation of seminal plasma into small- and large-solute fractions. sSP(–alb., –Fr.), albumin- and fructose-free sSP. (B) Fructose concentrations measured using the resorcinol assay in whole, small-solute, and large-solute hSP fractions from a pool of 10 hSP samples (pool C) and 10 individual donors. (C) HIV-1 infection and cell viability in hSP fractions. (Left) Infection by virus that contains the strain WEAU Env was performed in the indicated media by the approach outlined in Fig. 3C. In some large-solute samples, 30 mM fructose was supplemented. The fructose concentrations in all samples are shown. (Right) Cell viability was measured in the same experiment by an ATP assay. (D) HIV-1 inhibition in fractions of pooled hSP. Infection by isolate WEAU was measured in the presence of GRFT (60 nM), MAb 2G12 (20 μg/ml), or MAb PGT121 (3 μg/ml). Values are expressed as a percentage of the level of infection in each medium in the absence of inhibitors (shown in panel C). Error bars, SEM. *P* values were determined by a two-tailed *t* test. *, $P < 0.05$; **, $P < 0.005$. (E) (Left) Titration of GRFT effects on HIV-1 containing the strain 1053-07 Env in the indicated media. sSP was supplemented with 30 mM fructose. (Inset) Calculated IC_{50} and IC_{75} values of GRFT are shown. (Right) Infectivity, cell viability, and fructose concentrations in the different samples are shown.

trations of fructose in whole hSP and the small-solute fraction were similar, whereas this sugar was effectively removed from the retained large-solute fraction (Fig. 6B).

We examined the infectivity and inhibition of isolate WEAU in the small- and large-solute fractions of hSP from a pool of 10 donors. Relative to the results obtained with DMEM, infectivity was mildly increased in the small-solute fraction and mildly decreased in the large-solute fraction (Fig. 6C). These differences did not correspond with the effects of the samples on cell viability. Inhibition of infection by GRFT and MAb 2G12 was up to 10-fold higher in DMEM than in the small- and large-solute fractions of hSP, whereas similar levels of inhibition were observed for PGT121 in all media (Fig. 6D). Consistent with the findings mentioned above, supplementation of the large-solute fraction with fructose further rescued infection in the presence of GRFT 6-fold and modestly rescued infection in the presence of 2G12. In comparison, inhibition by

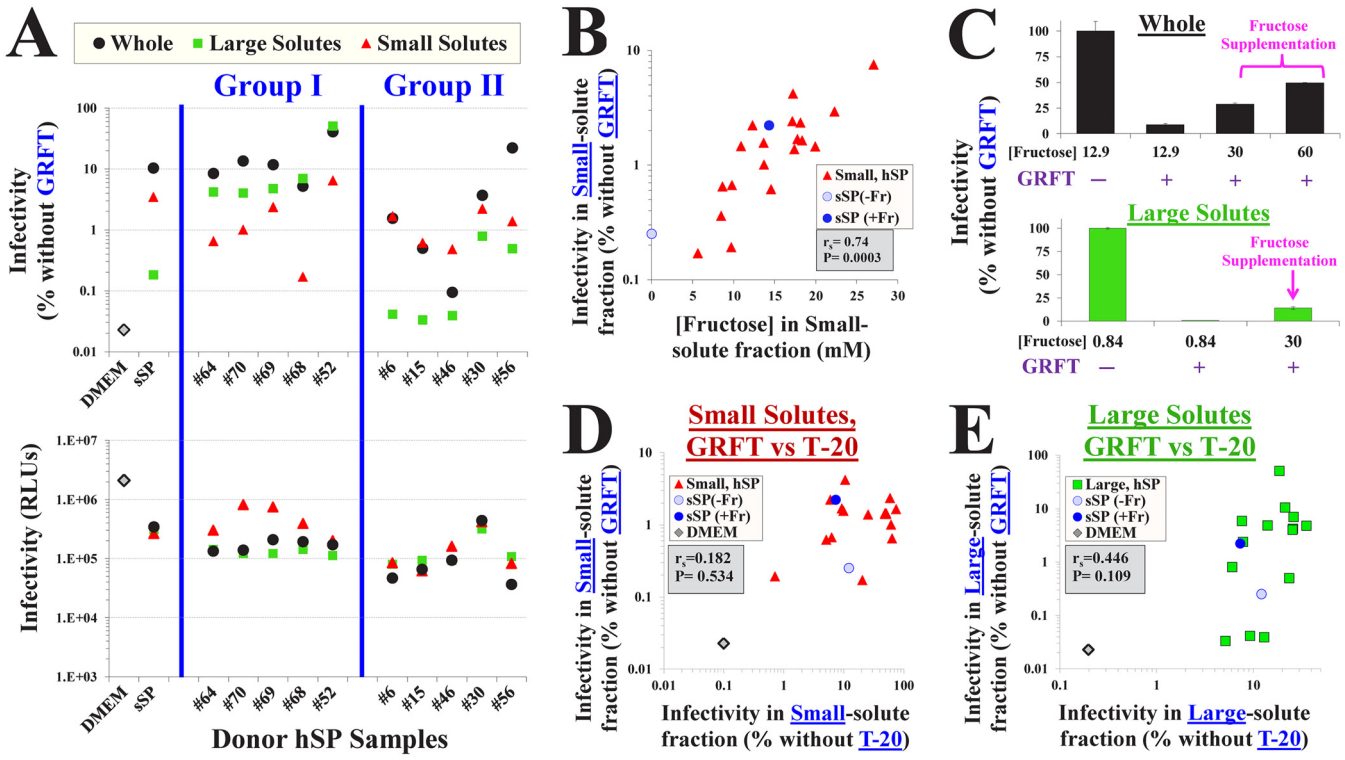

FIG 7 Fructose in human seminal plasma reduces HIV-1 inhibition by the lectin GRFT. (A) HIV-1 infection and GRFT inhibition in hSP fractions from different donors. (Bottom) Infection by virus containing the Env of isolate 1053-07 was measured in DMEM, sSP(+Fr) (15 mM), or whole hSP from individual donors and in the small- and large-solute fractions of all samples. (Top) Infection in the same samples was measured in the presence of 60 nM GRFT. Infection in the presence of GRFT is expressed as a percentage of the level of infection in its absence in the same sample. Group I donor samples showed greater effects of the large-solute fraction on GRFT inhibition than group II samples, whereas group II samples showed greater effects of the small-solute fraction than group I samples. (B) Relationship between the fructose concentration in the small-solute fraction of hSP samples and virus infectivity in the same samples in the presence of GRFT. (C) Supplementation of hSP samples with exogenous fructose rescues virus infectivity in the presence of GRFT. Fructose was added to whole SP or to the large-solute fraction from donor 30 to obtain the indicated concentrations of the saccharide. Error bars, SEM. (D, E) Comparison of HIV-1 inhibition by T-20 and GRFT in the small- and large-solute fractions of donor hSPs. Infectivity by virus containing the isolate 1053-07 Env was measured in the presence of T-20 (6 μM) or GRFT (60 nM) in hSP fractions from different donors. The infectivity measured in each donor sample in the presence of the inhibitors is compared. r_s, Spearman correlation coefficient. *P* values were determined by a two-tailed test.

PGT121 was unaffected by fructose supplementation. Titration of GRFT in the different media showed that the effect of fructose-containing sSP was similar to that of whole hSP, whereas both DMEM and fructose-free sSP allowed effective inhibition (Fig. 6E).

Semen fructose reduces HIV-1 inhibition by the lectin GRFT. To investigate the contribution of semen fructose to SP-mediated effects on GRFT inhibition, we analyzed whole and fractionated hSP samples from individual donors. Both the small- and large-solute fractions contributed to the resistance profile in whole hSP. In some samples, the large-solute fraction caused a greater rescue of infectivity in the presence of GRFT (group I in Fig. 7A) and could account for the effect of whole hSP. In other cases, the small-solute fraction caused a greater rescue of infection (group II in Fig. 7A). The differences in GRFT inhibition between hSP samples were not associated with the levels of infectivity measured in them (Fig. 7A, bottom). For example, samples from donors 64, 52, and 46 exhibited similar levels of infectivity in their small- and large-solute fractions but considerably different levels of GRFT inhibition. Importantly, the effect of the small-solute fraction of each sample on GRFT inhibition was highly correlated with the level of fructose that it contained (Fig. 7B). Virus inhibition was approximately 100-fold greater in samples that contained high concentrations of fructose than in samples that contained low concentrations. Consistent with this finding and the data shown in Fig. 6E, supplementation of a whole hSP sample that contained a low fructose concentration (from donor 30) with exogenous fructose effectively rescued infectivity in the presence of GRFT (Fig. 7C, top). Similarly, fructose

supplementation of the fructose-depleted large-solute fraction of this hSP effectively reduced GRFT inhibition (Fig. 7C, bottom).

To examine whether these effects are specific for the inhibitor, we compared the impact of the small- and large-solute fractions on GRFT with their impact on another agent that exhibits reduced potency in whole semen, the fusion inhibitor T-20 (Fig. 5F). In the presence of T-20, the small-solute fractions of the donor samples increased infectivity to different extents, ranging from no change to a 100-fold increase (Fig. 7D). Inhibition by T-20 and GRFT in sSP and hSP samples was significantly lower than that in DMEM. The effect of each small-solute sample on GRFT inhibition was not associated with its effect on T-20 inhibition. Consistent with this finding, the effects of the small-solute samples on T-20 inhibition were not correlated with their fructose content ($P = 0.27$ in a Spearman correlation test; data not shown). We also compared the potency of the two agents in the large-solute fractions (Fig. 7E). T-20 inhibition in the large-solute fractions of the sSP and hSP samples was 2 orders of magnitude lower than that in DMEM. Some large-solute samples showed considerable rescue from inhibition by both T-20 and GRFT; however, this relationship was not statistically significant ($P = 0.1$ in a Spearman correlation test).

Together, these data show that both large and small solutes in semen affect HIV-1 inhibition by GRFT. Different patient samples exerted different effects; in some cases, the profile in whole hSP could be explained by the effects of the small-solute fraction, whereas in others it could be explained by the effects of the large-solute fraction. For GRFT (but not for T-20), the effects of the small-solute fractions were largely determined by the fructose content. Depletion of small solutes from hSP increases GRFT inhibition, whereas replenishment of fructose reduces it. The effects of the large-solute fraction on the inhibitors spanned a range of up to 3 orders of magnitude in different samples. The inhibition profiles in the synthetic SP formulation reflected well the effects of the human semen samples and differed significantly from the inhibition profiles in DMEM. These results further emphasize the limited ability of cell culture media to accurately mimic the inhibitory profiles observed in human semen.

DISCUSSION

A wide array of BNAbs that target HIV-1 Env have been isolated and characterized over the past 3 decades (65). Several potent inhibitors of Env have also been developed as microbicides (reviewed in reference 66). The molecular basis for the interaction between many of these agents and Env has been thoroughly investigated. Additionally, inherent properties of the Envs have been described to explain the sensitivity profile of each virus strain (53, 67, 68). Nevertheless, one factor that significantly impacts the virus-inhibitor interaction has been relatively overlooked, the small-solute composition of the solvent. Different secretions serve as vehicles for the transmission of viruses; each contains a unique composition of salts and saccharides. Breast milk contains high levels of lactose (more than 200 mM) and a diversity of oligosaccharides. Saliva is uniquely hypotonic relative to other secretions (often less than 100 mOsm/l) (69, 70). Such diverse chemical environments can impact virus transmission and inhibition. In this work, we show that a unique chemical component of semen, fructose, affects HIV-1 recognition by inhibitory ligands. This effect is specific for a broadly acting and potent class of antiviral agents that target α1,2-linked mannose residues, which are abundant and conserved on HIV-1 and other pathogenic viruses.

Seminal plasma has evolved in mammals to maximize the viability of spermatozoa and their delivery to the oocyte. Semen is formed by the merging of glandular secretions in the ejaculatory duct, which initiates a rapid coagulation process (71). The coagulum then liquefies over minutes by proteolytic degradation (71, 72). Liquefied ejaculate is maintained in the vaginal cavity for several hours (24, 25). The buffering capacity and relatively large volume of semen neutralize the acidic pH of vaginal secretions and maintain virus infectivity (24). In healthy women, the ejaculate is then gradually replaced by low-pH vaginal secretions that inactivate the virus (24, 26, 27). Thus, during the time frame that viruses are infectious (i.e., transmissible), they are likely

exposed to semen (73, 74). It is during this time that mucosal antibodies and microbicides should inactivate the virus. However, the activity of these agents is reduced in semen (31, 35, 36, 62). Such effects can be explained, at least in part, by specific proteins unique to semen. Cationic polypeptide complexes in semen increase the rate of virus entry *in vitro*, thus nonspecifically reducing the potency of inhibitory agents (75, 76). Other large solutes in semen may sequester inhibitors (77). Here, we fractionated the donor samples into small- and large-solute components. In most samples, the large-solute fraction exerted significant effects on the potency of the inhibitors GRFT and T-20 (Fig. 7). In addition, we show that the small solutes of semen considerably reduce their potency; in half of the samples that we analyzed, the small solutes exerted a greater effect on GRFT efficacy than the large-solute fraction. The effect of the small-solute fraction on GRFT inhibition was determined by the concentration of fructose in the sample (Fig. 7B). Differences in fructose concentrations between donor samples may result from various contributions of the different organs to the ejaculate (mainly the prostate, seminal vesicles, testicles, and epididymis). For example, the volume of seminal vesicle secretions (the source of semen fructose) is affected by the duration of sexual abstinence (78) and inversely related to donor age (79). Other donor-specific properties may also affect semen parameters and composition (80). Such variation in semen glandular contributions can potentially explain the differences in inhibition profiles by the fusion inhibitor T-20. Several components of semen may affect T-20. The hydrophobic lipid-binding domain of this peptide at its C terminus (composed of Trp670, Trp672, and Phe673) likely allows binding to albumin (mainly derived from the prostate) and potentially other proteins in seminal plasma (81). Indeed, the protein content of hSP and sSP is higher than that of DMEM supplemented by 10% FCS. That the protein-free fraction of the simulant reduces T-20 inhibition (to a similar extent as the large-solute fraction; Fig. 7D and E) indicates that small solutes can also impact the efficacy of this peptide.

The high content of fructose in semen may also affect the attachment of HIV-1 (and possibly other viruses) to target cells. Myeloid cells at mucosal sites express dendritic cell-specific ICAM-grabbing nonintegrin (DC-SIGN). This cell-surface C-type lectin captures virions and mediates their transport to T cells in lymphoid organs (82, 83). Saccharides in other body fluids (e.g., breast milk) can reduce the binding of HIV-1 Env to DC-SIGN (84). It is plausible that semen fructose also affects DC-SIGN-mediated infection. The tools described in this work, which reduce the toxic effects of hSP, will likely facilitate investigations of the role of semen components in lectin-mediated infection.

Whereas our understanding of the molecular events associated with HIV-1 entry and postentry steps has improved over the past 3 decades, our knowledge of how they occur during sexual transmission and the impact of the chemical and molecular environment on them is still limited. A significant hurdle is imposed by the toxic effects of human semen on cells (28, 29, 33, 36). Multiple factors in semen are detrimental to cell viability, including the polyamines spermine, spermidine, and putrescine; their oxidation generates hydrogen peroxide and aminoaldehydes that are toxic to cells (85–87). In addition, the reactive oxygen species (ROS) generated by sperm and leukocytes in semen contribute to the oxidative stress (88). ROS are required for sperm cell capacitation and fertilization of the ovum (89); however, they can also damage sperm and other cells (90). Furthermore, aminoaldehydes and ROS can modify inhibitors by carbonylation, impairing their activity. To reduce toxic effects, we (i) used high-density cell cultures, which maintain greater viability in hSP than low-density cultures (Fig. 5B), and (ii) controlled the time of exposure to the medium; the entire entry process was allowed to occur for 75 min in semen in the presence of all factors (virus, inhibitor, cells, and 77.5% hSP). This time frame corresponds with the viability time of the virus in the vaginal cavity. After intercourse, semen increases the pH in the vaginal cavity from ~4 to ~7.2, which then decreases over the course of less than 2 h by acidic vaginal secretions (24). Once normal vaginal acidity is restored, viruses are inactivated. Thus, our time window of 75 min for exposure of virus to hSP reflects the

time frame in which the virus is functional in this environment. Despite the above-described measures, we expect that some toxicity is induced by many hSP samples. Reduced cell viability and effects on the inhibitors can potentially present spurious effects on inhibition. Several lines of evidence support the notion that the observed impacts of semen on inhibition cannot be substantially attributed to these factors but, rather, can be attributed to disruption of the Env-inhibitor interaction. First, the effect of each hSP sample on inhibition is not associated with its effects on virus infectivity or cell viability. For example, samples from donors 46 and 56 exerted the same effects on viability and infectivity but caused vastly different effects on GRFT inhibition (Fig. 5G). Second, we observed similar inhibition profiles in hSP and sSP, but these were distinct from those observed in DMEM. Third, the effects of hSP were inhibitor specific; the potencies of b12 and PGT121 were unaffected, whereas the potencies of 2G12, GRFT, and T-20 were significantly impaired (Fig. 5F).

It is noteworthy that fructose abrogates inhibition by GRFT more efficiently than that by 2G12; this was observed in DMEM (Fig. 1D), sSP (Fig. 4A), and hSP (Fig. 5F). Such effects may be attributed to the broader specificity of GRFT, which can also bind *N*-acetylglucosamine (38), whereas 2G12 does not bind this moiety (91). Efficient disruption of the interaction between GRFT and *N*-acetylglucosamine by fructose may render this inhibitor more sensitive to the effects of semen. In addition, the modestly lower affinity of GRFT to Env (relative to that of 2G12) may account for the greater competitive inhibition by fructose (92, 93). Supporting this notion is the finding that Env strains that are less sensitive to GRFT neutralization are more sensitive to the effects of fructose (Fig. 2E).

Our experimental design is based on the exposure of immobilized viruses to minimally diluted semen. A previous study by Zirafi and colleagues, which analyzed the effects of semen on HIV-1 neutralization, was based on dilution of the virus-hSP mix into cell cultures that contained the inhibitor (36). The two approaches analyze distinct effects of semen on inhibition and are complementary. The use of immobilized viruses is designed to eliminate the effects of semen on cell attachment, which can mask specific effects on the virus-inhibitor interaction. Accordingly, we observed no effects of hSP on the antibody b12 or PGT121; their binding to Env was likely not disrupted by a specific solute in semen. Our approach mimics the concentration of hSP to which virus and cells are exposed. The normal range for an ejaculate volume is 2 to 5 ml, whereas the volume of vaginal fluid is 0.5 to 1 ml (94), which explains the use of 77.5% hSP. Nevertheless, our approach assumes sufficient mixing of the semen and virus with the inhibitor before cells are encountered, which may be more limited *in vivo*. The dilution-based approach (36) mimics conditions under which the microbicide is contained in vaginal fluid and then semen-containing virus is deposited. It explains the effects of semen on the virus attachment step: semen reduced the efficacy of distinct antibodies, such as 2F5 and 2G12, to a similar extent, the changes corresponded with the effects of SEVI alone on efficacy of the antibodies (36). However, this approach does not reflect the proportions of semen and vaginal fluid after intercourse (normally, ~7:1) (22, 94), which may alter the interaction between Env and the inhibitor. Therefore, the two experimental approaches are complementary: one evaluates the effects of hSP on cell attachment and the other evaluates the effects of hSP on the interaction with the inhibitor. Both show a reduced effect of inhibitors in semen.

A vital tool that we applied to simulate semen-mediated virus transmission was a formulation of SP that contains the major small solutes in semen at their average physiological concentrations. The simulant is stable (i.e., does not precipitate) and nontoxic to cells for at least 6 h. The efficiency of HIV-1 entry in sSP resembled the average measured in hSP samples and differed from that measured in the cell culture medium (Fig. 7A). Furthermore, the potencies of the inhibitors (both T-20 and GRFT) in human and synthetic SPs were similar and differed (often by several orders of magnitude) from those measured in DMEM (Fig. 7D and E).

GRFT has been successfully tested in mice and nonhuman primates (20, 95, 96) and is currently applied in clinical trials as a vaginal or rectal microbicide to prevent the

transmission of HIV-1 and HPV. New methods have recently been developed to mass produce this agent in plants in combination with other high-mannose-targeting agents (97). Whereas GRFT is stable (98) and nontoxic to cells (42), our data suggest that its effective concentration is reduced by the ejaculate. Dilution by semen (99), the daily turnover of vaginal fluid (94), and sequestration by glycans on epithelial cells (42) will likely further reduce the activity of this agent. Since many strains exhibit intermediate sensitivity to GRFT, their neutralization *in vivo* will likely be impacted more considerably by semen fructose than the neutralization of strains that are highly sensitive to GRFT (Fig. 2E). Our findings suggest that it would be prudent to test the efficacy of these microbicides in the presence of semen simulants *in vitro* and in animal models as a preliminary step before clinical studies in humans.

MATERIALS AND METHODS

Antibodies, cells, and reagents. The reagents indicated below were obtained through the NIH AIDS Reagent Program, Division of AIDS, NIAID, NIH. Hermann Katinger kindly provided MAb 2G12 (10). The MAb 447-52D was contributed by Susan Zolla-Pazner (100). The MAb b12 was a kind gift from Dennis Burton (101, 102). Barry O'Keefe and James McMahon provided the recombinant His-tagged lectin griffithsin (98, 103). Robert Gallo contributed the T-cell lymphoma cell line H9 (104). The fusion inhibitor enfuvirtide (T-20) was provided by Roche. The International AIDS Vaccine Initiative (IAVI) Neutralizing Antibody Consortium kindly provided MAbs PGT121 and PGT126 (14, 105). The antiviral lectin *Galanthus nivalis* agglutinin (GNA) (9, 45) was purchased from Sigma-Aldrich (catalog number L8275). *Canis familiaris* thymus normal (Cf2Th) cells expressing CD4 and CCR5 (Cf2Th CD4$^+$ CCR5$^+$ cells) were provided by Joseph Sodroski (106). Human osteosarcoma (HOS) and human embryonic kidney (HEK) 293T cell lines were obtained from the American Type Culture Collection (ATCC). For all experiments performed in DMEM, the medium was supplemented with 10% fetal bovine serum.

Processing of donor seminal plasma. Semen samples from HIV-negative donors were provided to the In Vitro Fertilization and Reproductive Testing Laboratory at the University of Iowa Hospitals and Clinics. Deidentified donor seminal plasma intended for discarding were applied in this study (see below). Accordingly, this work was determined to be nonhuman subject research by the University of Iowa Human Use Review Board (Institutional Review Board number 201901845). Ejaculate was collected by masturbation into sterile containers, allowed to liquefy for 20 min at 37°C, and centrifuged at 3,000 rpm for 10 min to remove sperm and other cells. The supernatant (seminal plasma), which is normally discarded at this stage, was then collected, aliquoted, and frozen at −80°C until use. Information on all donor hSP samples, including age range, vasectomy status, days of sexual abstinence before collection, sample volume, and fructose concentration, is provided in Data Set S2 in the supplemental material. To separate small solutes (including fructose) from the larger SP components, 1 ml of each sample was filtered through a 3-kDa-MWCO membrane by centrifugation at 5,000 × *g* for 30 min and the filtrate was collected. To exchange the remaining small solutes in the retained fraction, 10 ml of albumin- and fructose-free sSP (see the composition below) was added and the sample was filtered through a 3-kDa-MWCO membrane by centrifugation. This process was repeated a second time, and the final retained fraction was collected and the volume was adjusted to the original volume (1 ml) using albumin- and fructose-free sSP.

Preparation of recombinant luciferase-expressing viruses. Env-expressing plasmids were generated by amplification of the *env* genes (nucleotides 5960 to 8904 of the HIV-1 genome) from the pCDNA3.1 expression vector and cloning of the product into the pSVIIIenv vector using the Infusion system (Clontech), as previously described (53, 107). Information about all Envs used in this study is provided in Data Set S1. Single-round, recombinant HIV-1 containing the Envs and expressing the firefly luciferase gene was generated by transfection of 293T cells using JetPrime reagent (Polyplus Inc.), as previously described (53). Briefly, 8.5×10^5 cells were seeded in each well of a 6-well plate and transfected the next day with 1.2 μg of the firefly luciferase-expressing construct pHIvec2.luc, 0.4 μg of the HIV-1 packaging construct pCMVΔP1ΔenvpA, and 0.2 μg and 0.4 μg of plasmids expressing HIV-1 Rev and Env, respectively. At 2 days after transfection, virus particles were pelleted from the supernatants by ultracentrifugation at 100,000 × *g* for 2 h at 12°C, resuspended in phosphate-buffered saline (PBS), and stored at −80°C until use. Viruses produced from H9 cells were generated in T75 flasks (7.0×10^6 cells per flask), using 12.4 μg of pHIvec2.luc, 4.1 μg of pCMVΔP1ΔenvpA, and 4.1 μg of a plasmid expressing HIV-1 Env.

Measurements of HIV-1 inhibition by antibodies and microbicides. Viruses suspended in DMEM were incubated at 37°C for 2 h in the absence or presence of HIV-1 inhibitors and different concentrations of fructose. Samples were then added to 96-well plates containing Cf2Th CD4$^+$ CCCR5$^+$ cells (3.0×10^4 per well), and the plates were incubated at 37°C for 72 h. All infectivity tests were performed with two replicate samples for each condition. Cells were lysed, and virus infection was measured by luminescence using luciferin reagent, as previously described (53). Inhibitor potency was calculated by the level of virus infection in the absence of inhibitor relative to the level of virus infection in its presence.

To measure infection in synthetic or human SP, viruses suspended in PBS were attached to 96-well protein-binding plates (PerkinElmer) by spinoculation at 2,000 × *g* for 2 h at 10°C. The plates were then blocked with DMEM for 16 h at 23°C. Plate-bound viruses were washed with Tris-buffered saline (150 mM NaCl, 20 mM Tris base, pH 7.5), and then 80 μl of SP (composed of 77.5 μl of SP and 2.5 μl of the

inhibitors or the PBS control) was added to each well. Samples were incubated at 37°C for 2 h, and 20 μl containing 6.0×10^4 Cf2Th CD4$^+$ CCR5$^+$ cells suspended in Tris-buffered saline was added to each well (final concentration of semen, 77.5%). Entry was allowed to proceed for 75 min at 37°C, the medium was removed, and trypsin was added to detach the cells. The cells were then resuspended in DMEM containing 11 μM the fusion inhibitor T-20 to prevent further infection and transferred to new 96-well plates. Virus infection and inhibitor potency were measured by luminescence 3 days later, as described above.

Measurement of inhibitor binding to HIV-1 Envs on cells and virus particles. Binding of antibodies and GRFT to HIV-1 Envs expressed on HOS cells was measured using a previously described cell-based ELISA system (53, 68, 106). Briefly, cells were seeded in 96-well plates (1.2×10^4 per well) and transfected with 60, 6, and 12 ng of plasmids expressing Env, Rev, and Tat, respectively, using the JetPrime transfection reagent. In all experiments, a negative-control plasmid containing a premature stop codon at amino acid position 46 of Env (according to the standard HXBc2 numbering) was used to quantify the background binding of each inhibitor to the cells. At 3 days after transfection, the cells were incubated in DMEM or sSP containing 0.5 μg/ml of the MAbs or 5 nM GRFT at 37°C for 45 min. All samples were then washed (in buffer containing 20 mg/ml bovine serum albumin [BSA], 1.8 mM $CaCl_2$, 1 mM $MgCl_2$, 25 mM Tris, pH 7.5, and 140 mM NaCl) and incubated in the same buffer supplemented with horseradish peroxidase (HRP)-conjugated goat anti-human immunoglobulin (Fisher Scientific) or mouse anti-His antibody (Proteintech) for 45 min. The cells were washed, and HRP enzyme activity was measured by light emission using chemiluminescence detection reagents with a Synergy H1 microplate reader (BioTek Instruments), as previously described (53). To measure inhibitor binding to viruses, purified virus stocks were diluted in PBS and attached to 96-well protein-binding plates by spinoculation at $2{,}000 \times g$ for 2 h at 10°C. The plates were then blocked with DMEM at 23°C for 16 h, and inhibitor binding was measured by ELISA, as described above.

Measurement of HIV-1 p24 antigen content by electrophoresis and Western blotting. Purified virus stocks (in PBS) were lysed by incubation with NP-40 buffer (0.5% NP-40, 0.5 M NaCl, 10 mM Tris, pH 7.5) for 1 h at 4°C with constant agitation. Samples were then loaded on 12% Tris-glycine polyacrylamide gels (Invitrogen), analyzed by SDS-PAGE, and transferred to polyvinylidene difluoride membranes. Polyclonal mouse anti-HIV-1 p24 antigen was used for probing the membranes, and a secondary (HRP-conjugated) goat anti-mouse IgG antibody was used for detection of the primary antibody. Band intensity was quantified by densitometry.

Preparation of sSP. The simulant of seminal plasma (sSP) formulation was prepared in 100-ml stocks and contained the following reagents: 0.71 mM sodium phosphate monobasic, 7.09 mM sodium phosphate dibasic, 20 mM sodium bicarbonate, 27.64 mM trisodium citrate, 12.18 mM potassium chloride, 15.7 mM potassium hydroxide, 6 mM glucose, 7 mM lactic acid, 7.5 mM urea, 4.5 mM magnesium chloride, 7 mM calcium chloride, 2 mM zinc chloride, and 5.04% BSA. The solution was adjusted to a pH of 7.7 and filtered through a 0.45-μm-pore-size membrane. Fructose was prepared at a stock concentration of 1.5 M in Tris-buffered saline (pH 7.7) and added to the simulant for a final concentration of 15 to 60 mM. The simulant formulation described by Owen and Katz was prepared as previously described (22). The buffering capacity of the formulations (in slyke units) was determined by the number of micromoles of HCl added to 1 ml of solution required to change the pH by 1 unit.

Effect of seminal plasma on cell viability and apoptosis induction. To measure cell viability, the ATP content in the samples was quantified using the CellTiter-Glo luminescent viability assay reagent (Promega). Cf2Th CD4$^+$ CCR5$^+$ cells were incubated in DMEM, sSP, or hSP at 37°C for different times, washed twice with DMEM, and further cultured in DMEM for 36 h at 37°C. The culture medium was removed, 100 μl of the CellTiter-Glo reagent was added to each well, and the samples were incubated for 10 min at 23°C. Luminescence was measured using a Synergy H1 luminometer.

To measure the induction of apoptosis, Cf2Th CD4$^+$ CCR5$^+$ cells (2×10^5 cells per 6-well plate well) were incubated for 75 min at 37°C with 1 ml of DMEM, sSP without fructose, sSP with 15 mM fructose, or DMEM supplemented with 4 μM the apoptosis-inducing agent staurosporine. The cells were then washed once with DMEM and further incubated in DMEM for 14 h at 37°C. The cells were subsequently detached from the plates using Accutase solution (Sigma), washed twice with PBS, and resuspended in 100 μl of binding buffer (150 mM NaCl, 5 mM $MgCl_2$, 5 mM KCl, 1.8 mM $CaCl_2$, 10 mM HEPES, pH 7.4). Five microliters of fluorescein isothiocyanate-conjugated annexin V antibody (BD Biosciences) was added to the cells, and the mixture was incubated at room temperature for 15 min. The sample was then supplemented with 400 μl of binding buffer and 1 μg/ml of propidium iodide, and the cells were analyzed by flow cytometry. The cells were gated by forward and side scatter to exclude debris.

Measurement of fructose concentration in human seminal plasma samples. Resorcinol- and indole-based colorimetric assays were used to measure fructose concentrations. The resorcinol agent was prepared by adding 33 ml of 12 M HCl to 67 ml of 45.4 mM resorcinol in water. Assay standards that contained different concentrations of fructose were prepared in Tris-buffered saline (150 mM NaCl, 20 mM Tris base, pH 7.5). Each SP sample was added to the resorcinol reagent at a 1:10 (vol/vol) dilution in a final volume of 330 μl, vortexed, and incubated for 3 min at 100°C. The samples were cooled at room temperature and added in duplicate to a 96-well plate, and the absorbance was read at 545 nm. For the indole-based assay, 5 μl of hSP or fructose standards was added to 50 μl of sterile water. Each sample was then supplemented with 12.5 μl of 63 mM zinc sulfate and 12.5 μl of 100 mM sodium hydroxide. Fifty microliters of each sample was added to 50 μl of 2 mM indole reagent (in water) and 500 μl of 12 M HCl, and the samples were incubated for 20 min at 50°C. The samples were then cooled on ice for 15 min, and the absorbance was read at 470 nm.

Statistical analysis. Two-tailed Spearman rank-order tests were used to evaluate the correlation between data variables (Spearman correlation coefficient [r_s]). *P* values of less than 0.05 were considered statistically significant. All experiments contained at least two replicate samples for each condition and were performed at least twice for validation. Standard errors of the means (SEM) were used to describe experimental variation within or between experiments, as indicated in the figure legends.

SUPPLEMENTAL MATERIAL

Supplemental material is available online only.

SUPPLEMENTAL FILE 1, XLSX file, 0.02 MB.

ACKNOWLEDGMENTS

We are grateful to Beatrice Hahn for the Envs of T/F viruses and Aloysius Klingelhutz for critical readings of the manuscript. We thank all donors who provided semen samples to this study.

This work was partly supported by the UIRF ICE Fund Award to H.H. J.J. was supported by an NIH Graduate Student Training Program Fellowship in Virology (grant NIH T32 AI007533-17).

We declare no competing interests.

REFERENCES

1. Cao L, Diedrich JK, Kulp DW, Pauthner M, He L, Park S-KR, Sok D, Su CY, Delahunty CM, Menis S, Andrabi R, Guenaga J, Georgeson E, Kubitz M, Adachi Y, Burton DR, Schief WR, Yates JR, Paulson JC. 2017. Global site-specific N-glycosylation analysis of HIV envelope glycoprotein. Nat Commun 8:14954. https://doi.org/10.1038/ncomms14954.
2. Go EP, Hewawasam G, Liao HX, Chen H, Ping LH, Anderson JA, Hua DC, Haynes BF, Desaire H. 2011. Characterization of glycosylation profiles of HIV-1 transmitted/founder envelopes by mass spectrometry. J Virol 85:8270–8284. https://doi.org/10.1128/JVI.05053-11.
3. McCaffrey RA, Saunders C, Hensel M, Stamatatos L. 2004. N-linked glycosylation of the V3 loop and the immunologically silent face of gp120 protects human immunodeficiency virus type 1 SF162 from neutralization by anti-gp120 and anti-gp41 antibodies. J Virol 78:3279–3295. https://doi.org/10.1128/jvi.78.7.3279-3295.2004.
4. Wei X, Decker JM, Wang S, Hui H, Kappes JC, Wu X, Salazar-Gonzalez JF, Salazar MG, Kilby JM, Saag MS, Komarova NL, Nowak MA, Hahn BH, Kwong PD, Shaw GM. 2003. Antibody neutralization and escape by HIV-1. Nature 422:307–312. https://doi.org/10.1038/nature01470.
5. Li Y, Luo L, Rasool N, Kang CY. 1993. Glycosylation is necessary for the correct folding of human immunodeficiency virus gp120 in CD4 binding. J Virol 67:584–588. https://doi.org/10.1128/JVI.67.1.584-588.1993.
6. Pal R, Hoke GM, Sarngadharan MG. 1989. Role of oligosaccharides in the processing and maturation of envelope glycoproteins of human immunodeficiency virus type 1. Proc Natl Acad Sci U S A 86:3384–3388. https://doi.org/10.1073/pnas.86.9.3384.
7. Moldt B, Rakasz EG, Schultz N, Chan-Hui PY, Swiderek K, Weisgrau KL, Piaskowski SM, Bergman Z, Watkins DI, Poignard P, Burton DR. 2012. Highly potent HIV-specific antibody neutralization in vitro translates into effective protection against mucosal SHIV challenge in vivo. Proc Natl Acad Sci U S A 109:18921–18925. https://doi.org/10.1073/pnas.1214785109.
8. Hessell AJ, Rakasz EG, Poignard P, Hangartner L, Landucci G, Forthal DN, Koff WC, Watkins DI, Burton DR. 2009. Broadly neutralizing human anti-HIV antibody 2G12 is effective in protection against mucosal SHIV challenge even at low serum neutralizing titers. PLoS Pathog 5:e1000433. https://doi.org/10.1371/journal.ppat.1000433.
9. Akkouh O, Ng TB, Singh SS, Yin C, Dan X, Chan YS, Pan W, Cheung RC. 2015. Lectins with anti-HIV activity: a review. Molecules 20:648–668. https://doi.org/10.3390/molecules20010648.
10. Trkola A, Purtscher M, Muster T, Ballaun C, Buchacher A, Sullivan N, Srinivasan K, Sodroski J, Moore JP, Katinger H. 1996. Human monoclonal antibody 2G12 defines a distinctive neutralization epitope on the gp120 glycoprotein of human immunodeficiency virus type 1. J Virol 70:1100–1108. https://doi.org/10.1128/JVI.70.2.1100-1108.1996.
11. Sanders RW, Venturi M, Schiffner L, Kalyanaraman R, Katinger H, Lloyd KO, Kwong PD, Moore JP. 2002. The mannose-dependent epitope for neutralizing antibody 2G12 on human immunodeficiency virus type 1 glycoprotein gp120. J Virol 76:7293–7305. https://doi.org/10.1128/jvi.76.14.7293-7305.2002.
12. Calarese DA, Scanlan CN, Zwick MB, Deechongkit S, Mimura Y, Kunert R, Zhu P, Wormald MR, Stanfield RL, Roux KH, Kelly JW, Rudd PM, Dwek RA, Katinger H, Burton DR, Wilson IA. 2003. Antibody domain exchange is an immunological solution to carbohydrate cluster recognition. Science 300:2065–2071. https://doi.org/10.1126/science.1083182.
13. Walker LM, Huber M, Doores KJ, Falkowska E, Pejchal R, Julien JP, Wang SK, Ramos A, Chan-Hui PY, Moyle M, Mitcham JL, Hammond PW, Olsen OA, Phung P, Fling S, Wong CH, Phogat S, Wrin T, Simek MD, Protocol G Principal Investigators, Koff WC, Wilson IA, Burton DR, Poignard P. 2011. Broad neutralization coverage of HIV by multiple highly potent antibodies. Nature 477:466–470. https://doi.org/10.1038/nature10373.
14. Pejchal R, Doores KJ, Walker LM, Khayat R, Huang PS, Wang SK, Stanfield RL, Julien JP, Ramos A, Crispin M, Depetris R, Katpally U, Marozsan A, Cupo A, Maloveste S, Liu Y, McBride R, Ito Y, Sanders RW, Ogohara C, Paulson JC, Feizi T, Scanlan CN, Wong CH, Moore JP, Olson WC, Ward AB, Poignard P, Schief WR, Burton DR, Wilson IA. 2011. A potent and broad neutralizing antibody recognizes and penetrates the HIV glycan shield. Science 334:1097–1103. https://doi.org/10.1126/science.1213256.
15. Mouquet H, Scharf L, Euler Z, Liu Y, Eden C, Scheid JF, Halper-Stromberg A, Gnanapragasam PN, Spencer DI, Seaman MS, Schuitemaker H, Feizi T, Nussenzweig MC, Bjorkman PJ. 2012. Complex-type N-glycan recognition by potent broadly neutralizing HIV antibodies. Proc Natl Acad Sci U S A 109:E3268–E3277. https://doi.org/10.1073/pnas.1217207109.
16. Julien JP, Sok D, Khayat R, Lee JH, Doores KJ, Walker LM, Ramos A, Diwanji DC, Pejchal R, Cupo A, Katpally U, Depetris RS, Stanfield RL, McBride R, Marozsan AJ, Paulson JC, Sanders RW, Moore JP, Burton DR, Poignard P, Ward AB, Wilson IA. 2013. Broadly neutralizing antibody PGT121 allosterically modulates CD4 binding via recognition of the HIV-1 gp120 V3 base and multiple surrounding glycans. PLoS Pathog 9:e1003342. https://doi.org/10.1371/journal.ppat.1003342.
17. Trkola A, Kuster H, Rusert P, Joos B, Fischer M, Leemann C, Manrique A, Huber M, Rehr M, Oxenius A, Weber R, Stiegler G, Vcelar B, Katinger H, Aceto L, Gunthard HF. 2005. Delay of HIV-1 rebound after cessation of antiretroviral therapy through passive transfer of human neutralizing antibodies. Nat Med 11:615–622. https://doi.org/10.1038/nm1244.
18. Mitchell CA, Ramessar K, O'Keefe BR. 2017. Antiviral lectins: selective inhibitors of viral entry. Antiviral Res 142:37–54. https://doi.org/10.1016/j.antiviral.2017.03.007.
19. Mori T, O'Keefe BR, Sowder RC, Bringans S, Gardella R, Berg S, Cochran P, Turpin JA, Buckheit RW, McMahon JB, Boyd MR. 2005. Isolation and characterization of griffithsin, a novel HIV-inactivating protein, from the red alga Griffithsia sp. J Biol Chem 280:9345–9353. https://doi.org/10.1074/jbc.M411122200.
20. Derby N, Lal M, Aravantinou M, Kizima L, Barnable P, Rodriguez A, Lai M, Wesenberg A, Ugaonkar S, Levendosky K, Mizenina O, Kleinbeck K,

Lifson JD, Peet MM, Lloyd Z, Benson M, Heneine W, O'Keefe BR, Robbiani M, Martinelli E, Grasperge B, Blanchard J, Gettie A, Teleshova N, Fernández-Romero JA, Zydowsky TM. 2018. Griffithsin carrageenan fast dissolving inserts prevent SHIV HSV-2 and HPV infections in vivo. Nat Commun 9:3881. https://doi.org/10.1038/s41467-018-06349-0.
21. Shaw GM, Hunter E. 2012. HIV transmission. Cold Spring Harb Perspect Med 2:a006965. https://doi.org/10.1101/cshperspect.a006965.
22. Owen DH, Katz DF. 2005. A review of the physical and chemical properties of human semen and the formulation of a semen simulant. J Androl 26:459–469. https://doi.org/10.2164/jandrol.04104.
23. Mitchell C, Paul K, Agnew K, Gaussman R, Coombs RW, Hitti J. 2011. Estimating volume of cervicovaginal secretions in cervicovaginal lavage fluid collected for measurement of genital HIV-1 RNA levels in women. J Clin Microbiol 49:735–736. https://doi.org/10.1128/JCM.00991-10.
24. Fox CA, Meldrum SJ, Watson BW. 1973. Continuous measurement by radio-telemetry of vaginal pH during human coitus. J Reprod Fertil 33:69–75. https://doi.org/10.1530/jrf.0.0330069.
25. Ricci LR, Hoffman SA. 1982. Prostatic acid phosphatase and sperm in the post-coital vagina. Ann Emerg Med 11:530–534. https://doi.org/10.1016/s0196-0644(82)80424-1.
26. Ongradi J, Ceccherini-Nelli L, Pistello M, Specter S, Bendinelli M. 1990. Acid sensitivity of cell-free and cell-associated HIV-1: clinical implications. AIDS Res Hum Retroviruses 6:1433–1436. https://doi.org/10.1089/aid.1990.6.1433.
27. Tyssen D, Wang YY, Hayward JA, Agius PA, DeLong K, Aldunate M, Ravel J, Moench TR, Cone RA, Tachedjian G. 2018. Anti-HIV-1 activity of lactic acid in human cervicovaginal fluid. mSphere 3:e00055-18. https://doi.org/10.1128/mSphere.00055-18.
28. Munch J, Rucker E, Standker L, Adermann K, Goffinet C, Schindler M, Wildum S, Chinnadurai R, Rajan D, Specht A, Gimenez-Gallego G, Sanchez PC, Fowler DM, Koulov A, Kelly JW, Mothes W, Grivel JC, Margolis L, Keppler OT, Forssmann WG, Kirchhoff F. 2007. Semen-derived amyloid fibrils drastically enhance HIV infection. Cell 131:1059–1071. https://doi.org/10.1016/j.cell.2007.10.014.
29. Sabatte J, Ceballos A, Raiden S, Vermeulen M, Nahmod K, Maggini J, Salamone G, Salomon H, Amigorena S, Geffner J. 2007. Human seminal plasma abrogates the capture and transmission of human immunodeficiency virus type 1 to CD4$^+$ T cells mediated by DC-SIGN. J Virol 81:13723–13734. https://doi.org/10.1128/JVI.01079-07.
30. Martellini JA, Cole AL, Venkataraman N, Quinn GA, Svoboda P, Gangrade BK, Pohl J, Sorensen OE, Cole AM. 2009. Cationic polypeptides contribute to the anti-HIV-1 activity of human seminal plasma. FASEB J 23:3609–3618. https://doi.org/10.1096/fj.09-131961.
31. Neurath AR, Strick N, Li YY. 2006. Role of seminal plasma in the anti-HIV-1 activity of candidate microbicides. BMC Infect Dis 6:150. https://doi.org/10.1186/1471-2334-6-150.
32. French KC, Roan NR, Makhatadze GI. 2014. Structural characterization of semen coagulum-derived SEM1(86-107) amyloid fibrils that enhance HIV-1 infection. Biochemistry 53:3267–3277. https://doi.org/10.1021/bi500427r.
33. Kim K-A, Yolamanova M, Zirafi O, Roan NR, Staendker L, Forssmann W-G, Burgener A, Dejucq-Rainsford N, Hahn BH, Shaw GM, Greene WC, Kirchhoff F, Münch J. 2010. Semen-mediated enhancement of HIV infection is donor-dependent and correlates with the levels of SEVI. Retrovirology 7:55. https://doi.org/10.1186/1742-4690-7-55.
34. Lippold S, Braun B, Krüger F, Harms M, Müller JA, Groß R, Münch J, von Einem J. 2019. Natural inhibitor of human cytomegalovirus in human seminal plasma. J Virol 93:e01855-18. https://doi.org/10.1128/JVI.01855-18.
35. Patel S, Hazrati E, Cheshenko N, Galen B, Yang H, Guzman E, Wang R, Herold BC, Keller MJ. 2007. Seminal plasma reduces the effectiveness of topical polyanionic microbicides. J Infect Dis 196:1394–1402. https://doi.org/10.1086/522606.
36. Zirafi O, Kim KA, Roan NR, Kluge SF, Muller JA, Jiang S, Mayer B, Greene WC, Kirchhoff F, Munch J. 2014. Semen enhances HIV infectivity and impairs the antiviral efficacy of microbicides. Sci Transl Med 6:262ra157. https://doi.org/10.1126/scitranslmed.3009634.
37. Doores KJ, Fulton Z, Hong V, Patel MK, Scanlan CN, Wormald MR, Finn MG, Burton DR, Wilson IA, Davis BG. 2010. A nonself sugar mimic of the HIV glycan shield shows enhanced antigenicity. Proc Natl Acad Sci U S A 107:17107–17112. https://doi.org/10.1073/pnas.1002717107.
38. Ziółkowska NE, Shenoy SR, O'Keefe BR, Wlodawer A. 2007. Crystallographic studies of the complexes of antiviral protein griffithsin with glucose and N-acetylglucosamine. Protein Sci 16:1485–1489. https://doi.org/10.1110/ps.072889407.
39. Haim H, Salas I, Sodroski J. 2013. Proteolytic processing of the human immunodeficiency virus envelope glycoprotein precursor decreases conformational flexibility. J Virol 87:1884–1889. https://doi.org/10.1128/JVI.02765-12.
40. Lusvarghi S, Bewley CA. 2016. Griffithsin: an antiviral lectin with outstanding therapeutic potential. Viruses 8:E296. https://doi.org/10.3390/v8100296.
41. Alexandre KB, Gray ES, Lambson BE, Moore PL, Choge IA, Mlisana K, Karim SSA, McMahon J, O'Keefe B, Chikwamba R, Morris L. 2010. Mannose-rich glycosylation patterns on HIV-1 subtype C gp120 and sensitivity to the lectins, griffithsin, cyanovirin-N and scytovirin. Virology 402:187–196. https://doi.org/10.1016/j.virol.2010.03.021.
42. Kouokam JC, Huskens D, Schols D, Johannemann A, Riedell SK, Walter W, Walker JM, Matoba N, O'Keefe BR, Palmer KE. 2011. Investigation of griffithsin's interactions with human cells confirms its outstanding safety and efficacy profile as a microbicide candidate. PLoS One 6:e22635. https://doi.org/10.1371/journal.pone.0022635.
43. Moulaei T, Shenoy SR, Giomarelli B, Thomas C, McMahon JB, Dauter Z, O'Keefe BR, Wlodawer A. 2010. Monomerization of viral entry inhibitor griffithsin elucidates the relationship between multivalent binding to carbohydrates and anti-HIV activity. Structure 18:1104–1115. https://doi.org/10.1016/j.str.2010.05.016.
44. Xue J, Gao Y, Hoorelbeke B, Kagiampakis I, Zhao B, Demeler B, Balzarini J, Liwang PJ. 2012. The role of individual carbohydrate-binding sites in the function of the potent anti-HIV lectin griffithsin. Mol Pharm 9:2613–2625. https://doi.org/10.1021/mp300194b.
45. Hu B, Du T, Li C, Luo S, Liu Y, Huang X, Hu Q. 2015. Sensitivity of transmitted and founder human immunodeficiency virus type 1 envelopes to carbohydrate-binding agents griffithsin, cyanovirin-N and Galanthus nivalis agglutinin. J Gen Virol 96:3660–3666. https://doi.org/10.1099/jgv.0.000299.
46. Raska M, Takahashi K, Czernekova L, Zachova K, Hall S, Moldoveanu Z, Elliott MC, Wilson L, Brown R, Jancova D, Barnes S, Vrbkova J, Tomana M, Smith PD, Mestecky J, Renfrow MB, Novak J. 2010. Glycosylation patterns of HIV-1 gp120 depend on the type of expressing cells and affect antibody recognition. J Biol Chem 285:20860–20869. https://doi.org/10.1074/jbc.M109.085472.
47. Kong L, Sheppard NC, Stewart-Jones GB, Robson CL, Chen H, Xu X, Krashias G, Bonomelli C, Scanlan CN, Kwong PD, Jeffs SA, Jones IM, Sattentau QJ. 2010. Expression-system-dependent modulation of HIV-1 envelope glycoprotein antigenicity and immunogenicity. J Mol Biol 403:131–147. https://doi.org/10.1016/j.jmb.2010.08.033.
48. Jan M, Upadhyay C, Alcami Pertejo J, Hioe CE, Arora SK. 2018. Heterogeneity in glycan composition on the surface of HIV-1 envelope determines virus sensitivity to lectins. PLoS One 13:e0194498. https://doi.org/10.1371/journal.pone.0194498.
49. Alexandre KB, Gray ES, Pantophlet R, Moore PL, McMahon JB, Chakauya E, O'Keefe BR, Chikwamba R, Morris L. 2011. Binding of the mannose-specific lectin, griffithsin, to HIV-1 gp120 exposes the CD4-binding site. J Virol 85:9039–9050. https://doi.org/10.1128/JVI.02675-10.
50. Rastogi R, Su J, Mahalingam A, Clark J, Sung S, Hope T, Kiser PF. 2016. Engineering and characterization of simplified vaginal and seminal fluid simulants. Contraception 93:337–346. https://doi.org/10.1016/j.contraception.2015.11.008.
51. Allen RD, Roberts TK. 1986. The relationship between the immunosuppressive and cytotoxic effects of human seminal plasma. Am J Reprod Immunol Microbiol 11:59–64. https://doi.org/10.1111/j.1600-0897.1986.tb00030.x.
52. Perdomo MF, Hosia W, Jejcic A, Corthals GL, Vahlne A. 2012. Human serum protein enhances HIV-1 replication and up-regulates the transcription factor AP-1. Proc Natl Acad Sci U S A 109:17639–17644. https://doi.org/10.1073/pnas.1206893109.
53. Johnson J, Zhai Y, Salimi H, Espy N, Eichelberger N, DeLeon O, O'Malley Y, Courter J, Smith AB, III, Madani N, Sodroski J, Haim H. 2017. Induction of a tier-1-like phenotype in diverse tier-2 isolates by agents that guide HIV-1 Env to perturbation-sensitive, nonnative states. J Virol 91:e00174-17. https://doi.org/10.1128/JVI.00174-17.
54. Kassa A, Finzi A, Pancera M, Courter JR, Smith AB, III, Sodroski J. 2009. Identification of a human immunodeficiency virus type 1 envelope glycoprotein variant resistant to cold inactivation. J Virol 83:4476–4488. https://doi.org/10.1128/JVI.02110-08.
55. Kordy K, Elliott J, Tanner K, Johnson EJ, McGowan IM, Anton PA. 2018. Human semen or seminal plasma does not enhance HIV-1BaL ex vivo

infection of human colonic explants. AIDS Res Hum Retroviruses 34:459–466. https://doi.org/10.1089/AID.2017.0118.
56. Introini A, Bostrom S, Bradley F, Gibbs A, Glaessgen A, Tjernlund A, Broliden K. 2017. Seminal plasma induces inflammation and enhances HIV-1 replication in human cervical tissue explants. PLoS Pathog 13:e1006402. https://doi.org/10.1371/journal.ppat.1006402.
57. Arsenault GP, Yaphe W. 1966. Fructose-resorcinol-hydrochloric acid test for detection and determination of acetaldehyde. Anal Chem 38:503–504. https://doi.org/10.1021/ac60235a036.
58. World Health Organization. 2001. Laboratory manual of the WHO for the examination of human semen and sperm-cervical mucus interaction. Ann Ist Super Sanita 37:I–XII, 1–123. (In Italian).
59. Goldstein M, Schlossberg S. 1988. Men with congenital absence of the vas deferens often have seminal vesicles. J Urol 140:85–86. https://doi.org/10.1016/s0022-5347(17)41493-5.
60. Wild C, Oas T, McDanal C, Bolognesi D, Matthews T. 1992. A synthetic peptide inhibitor of human immunodeficiency virus replication: correlation between solution structure and viral inhibition. Proc Natl Acad Sci U S A 89:10537–10541. https://doi.org/10.1073/pnas.89.21.10537.
61. Haim H, Steiner I, Panet A. 2007. Time frames for neutralization during the human immunodeficiency virus type 1 entry phase, as monitored in synchronously infected cell cultures. J Virol 81:3525–3534. https://doi.org/10.1128/JVI.02293-06.
62. Tan S, Lu L, Li L, Liu J, Oksov Y, Lu H, Jiang S, Liu S. 2013. Polyanionic candidate microbicides accelerate the formation of semen-derived amyloid fibrils to enhance HIV-1 infection. PLoS One 8:e59777. https://doi.org/10.1371/journal.pone.0059777.
63. Munch J, Sauermann U, Yolamanova M, Raue K, Stahl-Hennig C, Kirchhoff F. 2013. Effect of semen and seminal amyloid on vaginal transmission of simian immunodeficiency virus. Retrovirology 10:148. https://doi.org/10.1186/1742-4690-10-148.
64. Madison MN, Roller RJ, Okeoma CM. 2014. Human semen contains exosomes with potent anti-HIV-1 activity. Retrovirology 11:102. https://doi.org/10.1186/s12977-014-0102-z.
65. Wibmer CK, Moore PL, Morris L. 2015. HIV broadly neutralizing antibody targets. Curr Opin HIV AIDS 10:135–143. https://doi.org/10.1097/COH.0000000000000153.
66. Lederman MM, Offord RE, Hartley O. 2006. Microbicides and other topical strategies to prevent vaginal transmission of HIV. Nat Rev Immunol 6:371–382. https://doi.org/10.1038/nri1848.
67. Montefiori DC, Roederer M, Morris L, Seaman MS. 2018. Neutralization tiers of HIV-1. Curr Opin HIV AIDS 13:128–136. https://doi.org/10.1097/COH.0000000000000442.
68. Haim H, Strack B, Kassa A, Madani N, Wang L, Courter JR, Princiotto A, McGee K, Pacheco B, Seaman MS, Smith AB, III, Sodroski J. 2011. Contribution of intrinsic reactivity of the HIV-1 envelope glycoproteins to CD4-independent infection and global inhibitor sensitivity. PLoS Pathog 7:e1002101. https://doi.org/10.1371/journal.ppat.1002101.
69. Baron S, Poast J, Richardson CJ, Nguyen D, Cloyd M. 2000. Oral transmission of human immunodeficiency virus by infected seminal fluid and milk: a novel mechanism. J Infect Dis 181:498–504. https://doi.org/10.1086/315251.
70. Etzold S, Bode L. 2014. Glycan-dependent viral infection in infants and the role of human milk oligosaccharides. Curr Opin Virol 7:101–107. https://doi.org/10.1016/j.coviro.2014.06.005.
71. Duncan MW, Thompson HS. 2007. Proteomics of semen and its constituents. Proteomics Clin Appl 1:861–875. https://doi.org/10.1002/prca.200700228.
72. Emami N, Deperthes D, Malm J, Diamandis EP. 2008. Major role of human KLK14 in seminal clot liquefaction. J Biol Chem 283:19561–19569. https://doi.org/10.1074/jbc.M801194200.
73. Miller CJ, Li Q, Abel K, Kim E-Y, Ma Z-M, Wietgrefe S, La Franco-Scheuch L, Compton L, Duan L, Shore MD, Zupancic M, Busch M, Carlis J, Wolinsky S, Wolinksy S, Haase AT. 2005. Propagation and dissemination of infection after vaginal transmission of simian immunodeficiency virus. J Virol 79:9217–9227. https://doi.org/10.1128/JVI.79.14.9217-9227.2005.
74. Hu J, Gardner MB, Miller CJ. 2000. Simian immunodeficiency virus rapidly penetrates the cervicovaginal mucosa after intravaginal inoculation and infects intraepithelial dendritic cells. J Virol 74:6087–6095. https://doi.org/10.1128/jvi.74.13.6087-6095.2000.
75. Roan NR, Munch J, Arhel N, Mothes W, Neidleman J, Kobayashi A, Smith-McCune K, Kirchhoff F, Greene WC. 2009. The cationic properties of SEVI underlie its ability to enhance human immunodeficiency virus infection. J Virol 83:73–80. https://doi.org/10.1128/JVI.01366-08.
76. Roan NR, Muller JA, Liu H, Chu S, Arnold F, Sturzel CM, Walther P, Dong M, Witkowska HE, Kirchhoff F, Munch J, Greene WC. 2011. Peptides released by physiological cleavage of semen coagulum proteins form amyloids that enhance HIV infection. Cell Host Microbe 10:541–550. https://doi.org/10.1016/j.chom.2011.10.010.
77. Vallner JJ. 1977. Binding of drugs by albumin and plasma protein. J Pharm Sci 66:447–465. https://doi.org/10.1002/jps.2600660402.
78. Cooper TG, Keck C, Oberdieck U, Nieschlag E. 1993. Effects of multiple ejaculations after extended periods of sexual abstinence on total, motile and normal sperm numbers, as well as accessory gland secretions, from healthy normal and oligozoospermic men. Hum Reprod 8:1251–1258. https://doi.org/10.1093/oxfordjournals.humrep.a138236.
79. Elzanaty S. 2007. Association between age and epididymal and accessory sex gland function and their relation to sperm motility. Arch Androl 53:149–156. https://doi.org/10.1080/01485010701225667.
80. Keel BA. 2006. Within- and between-subject variation in semen parameters in infertile men and normal semen donors. Fertil Steril 85:128–134. https://doi.org/10.1016/j.fertnstert.2005.06.048.
81. Sivertsen A, Isaksson J, Leiros HK, Svenson J, Svendsen JS, Brandsdal BO. 2014. Synthetic cationic antimicrobial peptides bind with their hydrophobic parts to drug site II of human serum albumin. BMC Struct Biol 14:4. https://doi.org/10.1186/1472-6807-14-4.
82. Geijtenbeek TB, Kwon DS, Torensma R, van Vliet SJ, van Duijnhoven GC, Middel J, Cornelissen IL, Nottet HS, KewalRamani VN, Littman DR, Figdor CG, van Kooyk Y. 2000. DC-SIGN, a dendritic cell-specific HIV-1-binding protein that enhances trans-infection of T cells. Cell 100:587–597. https://doi.org/10.1016/s0092-8674(00)80694-7.
83. Cavrois M, Neidleman J, Kreisberg JF, Greene WC. 2007. In vitro derived dendritic cells trans-infect CD4 T cells primarily with surface-bound HIV-1 virions. PLoS Pathog 3:e4. https://doi.org/10.1371/journal.ppat.0030004.
84. Naarding MA, Ludwig IS, Groot F, Berkhout B, Geijtenbeek TB, Pollakis G, Paxton WA. 2005. Lewis X component in human milk binds DC-SIGN and inhibits HIV-1 transfer to $CD4^+$ T lymphocytes. J Clin Invest 115:3256–3264. https://doi.org/10.1172/JCI25105.
85. Klebanoff SJ, Kazazi F. 1995. Inactivation of human immunodeficiency virus type 1 by the amine oxidase-peroxidase system. J Clin Microbiol 33:2054–2057. https://doi.org/10.1128/JCM.33.8.2054-2057.1995.
86. Maayan R, Zukerman Z, Shohat B. 1995. Oxidation of polyamines in human seminal plasma: a possible role in immunological infertility. Arch Androl 34:95–99. https://doi.org/10.3109/01485019508987836.
87. Pegg AE. 2013. Toxicity of polyamines and their metabolic products. Chem Res Toxicol 26:1782–1800. https://doi.org/10.1021/tx400316s.
88. Aitken RJ, Buckingham DW, Brindle J, Gomez E, Baker HW, Irvine DS. 1995. Analysis of sperm movement in relation to the oxidative stress created by leukocytes in washed sperm preparations and seminal plasma. Hum Reprod 10:2061–2071. https://doi.org/10.1093/oxfordjournals.humrep.a136237.
89. Aitken RJ, Whiting S, De Iuliis GN, McClymont S, Mitchell LA, Baker MA. 2012. Electrophilic aldehydes generated by sperm metabolism activate mitochondrial reactive oxygen species generation and apoptosis by targeting succinate dehydrogenase. J Biol Chem 287:33048–33060. https://doi.org/10.1074/jbc.M112.366690.
90. Homa ST, Vessey W, Perez-Miranda A, Riyait T, Agarwal A. 2015. Reactive oxygen species (ROS) in human semen: determination of a reference range. J Assist Reprod Genet 32:757–764. https://doi.org/10.1007/s10815-015-0454-x.
91. Scanlan CN, Pantophlet R, Wormald MR, Ollmann Saphire E, Stanfield R, Wilson IA, Katinger H, Dwek RA, Rudd PM, Burton DR. 2002. The broadly neutralizing anti-human immunodeficiency virus type 1 antibody 2G12 recognizes a cluster of alpha1→2 mannose residues on the outer face of gp120. J Virol 76:7306–7321. https://doi.org/10.1128/jvi.76.14.7306-7321.2002.
92. West AP, Jr, Galimidi RP, Foglesong CP, Gnanapragasam PN, Huey-Tubman KE, Klein JS, Suzuki MD, Tiangco NE, Vielmetter J, Bjorkman PJ. 2009. Design and expression of a dimeric form of human immunodeficiency virus type 1 antibody 2G12 with increased neutralization potency. J Virol 83:98–104. https://doi.org/10.1128/JVI.01564-08.
93. O'Keefe BR, Giomarelli B, Barnard DL, Shenoy SR, Chan PKS, McMahon JB, Palmer KE, Barnett BW, Meyerholz DK, Wohlford-Lenane CL, McCray PB, Jr. 2010. Broad-spectrum in vitro activity and in vivo efficacy of the antiviral protein griffithsin against emerging viruses of the family Coronaviridae. J Virol 84:2511–2521. https://doi.org/10.1128/JVI.02322-09.

94. Owen DH, Katz DF. 1999. A vaginal fluid simulant. Contraception 59:91–95. https://doi.org/10.1016/s0010-7824(99)00010-4.
95. Girard L, Birse K, Holm JB, Gajer P, Humphrys MS, Garber D, Guenthner P, Noel-Romas L, Abou M, McCorrister S, Westmacott G, Wang L, Rohan LC, Matoba N, McNicholl J, Palmer KE, Ravel J, Burgener AD. 2018. Impact of the griffithsin anti-HIV microbicide and placebo gels on the rectal mucosal proteome and microbiome in non-human primates. Sci Rep 8:8059. https://doi.org/10.1038/s41598-018-26313-8.
96. Nixon B, Stefanidou M, Mesquita PM, Fakioglu E, Segarra T, Rohan L, Halford W, Palmer KE, Herold BC. 2013. Griffithsin protects mice from genital herpes by preventing cell-to-cell spread. J Virol 87:6257–6269. https://doi.org/10.1128/JVI.00012-13.
97. Vamvaka E, Farré G, Molinos-Albert LM, Evans A, Canela-Xandri A, Twyman RM, Carrillo J, Ordóñez RA, Shattock RJ, O'Keefe BR, Clotet B, Blanco J, Khush GS, Christou P, Capell T. 2018. Unexpected synergistic HIV neutralization by a triple microbicide produced in rice endosperm. Proc Natl Acad Sci U S A 115:E7854–E7862. https://doi.org/10.1073/pnas.1806022115.
98. Emau P, Tian B, O'Keefe BR, Mori T, McMahon JB, Palmer KE, Jiang Y, Bekele G, Tsai CC. 2007. Griffithsin, a potent HIV entry inhibitor, is an excellent candidate for anti-HIV microbicide. J Med Primatol 36:244–253. https://doi.org/10.1111/j.1600-0684.2007.00242.x.
99. Levitas E, Lunenfeld E, Weisz N, Friger M, Potashnik G. 2007. Relationship between age and semen parameters in men with normal sperm concentration: analysis of 6022 semen samples. Andrologia 39:45–50. https://doi.org/10.1111/j.1439-0272.2007.00761.x.
100. Gorny MK, Conley AJ, Karwowska S, Buchbinder A, Xu JY, Emini EA, Koenig S, Zolla-Pazner S. 1992. Neutralization of diverse human immunodeficiency virus type 1 variants by an anti-V3 human monoclonal antibody. J Virol 66:7538–7542. https://doi.org/10.1128/JVI.66.12.7538-7542.1992.
101. Zhou T, Xu L, Dey B, Hessell AJ, Van Ryk D, Xiang SH, Yang X, Zhang MY, Zwick MB, Arthos J, Burton DR, Dimitrov DS, Sodroski J, Wyatt R, Nabel GJ, Kwong PD. 2007. Structural definition of a conserved neutralization epitope on HIV-1 gp120. Nature 445:732–737. https://doi.org/10.1038/nature05580.
102. Burton DR, Pyati J, Koduri R, Sharp SJ, Thornton GB, Parren PW, Sawyer LS, Hendry RM, Dunlop N, Nara PL, Lamacchia M, Garratty E, Stiehm ER, Bryson J, Cao Y, Moore JP, Ho DD, Barbas CF, III. 1994. Efficient neutralization of primary isolates of HIV-1 by a recombinant human monoclonal antibody. Science 266:1024–1027. https://doi.org/10.1126/science.7973652.
103. Ziółkowska NE, O'Keefe BR, Mori T, Zhu C, Giomarelli B, Vojdani F, Palmer KE, McMahon JB, Wlodawer A. 2006. Domain-swapped structure of the potent antiviral protein griffithsin and its mode of carbohydrate binding. Structure 14:1127–1135. https://doi.org/10.1016/j.str.2006.05.017.
104. Mann DL, O'Brien SJ, Gilbert DA, Reid Y, Popovic M, Read-Connole E, Gallo RC, Gazdar AF. 1989. Origin of the HIV-susceptible human $CD4^+$ cell line H9. AIDS Res Hum Retroviruses 5:253–255. https://doi.org/10.1089/aid.1989.5.253.
105. Walker LM, Phogat SK, Chan-Hui PY, Wagner D, Phung P, Goss JL, Wrin T, Simek MD, Fling S, Mitcham JL, Lehrman JK, Priddy FH, Olsen OA, Frey SM, Hammond PW, Protocol G Principal Investigators, Kaminsky S, Zamb T, Moyle M, Koff WC, Poignard P, Burton DR. 2009. Broad and potent neutralizing antibodies from an African donor reveal a new HIV-1 vaccine target. Science 326:285–289. https://doi.org/10.1126/science.1178746.
106. Haim H, Si Z, Madani N, Wang L, Courter JR, Princiotto A, Kassa A, DeGrace M, McGee-Estrada K, Mefford M, Gabuzda D, Smith AB, III, Sodroski J. 2009. Soluble CD4 and $CD4^-$ mimetic compounds inhibit HIV-1 infection by induction of a short-lived activated state. PLoS Pathog 5:e1000360. https://doi.org/10.1371/journal.ppat.1000360.
107. DeLeon O, Hodis H, O'Malley Y, Johnson J, Salimi H, Zhai Y, Winter E, Remec C, Eichelberger N, Van Cleave B, Puliadi R, Harrington RD, Stapleton JT, Haim H. 2017. Accurate predictions of population-level changes in sequence and structural properties of HIV-1 Env using a volatility-controlled diffusion model. PLoS Biol 15:e2001549. https://doi.org/10.1371/journal.pbio.2001549.